

THIS REPORT HAS BEEN DELIMITED  
AND CLEARED FOR PUBLIC RELEASE  
UNDER DOD DIRECTIVE 5200.20 AND  
NO RESTRICTIONS ARE IMPOSED UPON  
ITS USE AND DISCLOSURE.

DISTRIBUTION STATEMENT A

APPROVED FOR PUBLIC RELEASE;  
DISTRIBUTION UNLIMITED.

# Armed Services Technical Information Agency

Because of our limited supply, you are requested to return this copy WHEN IT HAS SERVED YOUR PURPOSE so that it may be made available to other requesters. Your cooperation will be appreciated.

# AD

# 40814

NOTICE: WHEN GOVERNMENT OR OTHER DRAWINGS, SPECIFICATIONS OR OTHER DATA ARE USED FOR ANY PURPOSE OTHER THAN IN CONNECTION WITH A DEFINITELY RELATED GOVERNMENT PROCUREMENT OPERATION, THE U. S. GOVERNMENT THEREBY INCURS NO RESPONSIBILITY, NOR ANY OBLIGATION WHATSOEVER; AND THE FACT THAT THE GOVERNMENT MAY HAVE FORMULATED, FURNISHED, OR IN ANY WAY SUPPLIED THE SAID DRAWINGS, SPECIFICATIONS, OR OTHER DATA IS NOT TO BE REGARDED BY IMPLICATION OR OTHERWISE AS IN ANY MANNER LICENSING THE HOLDER OR ANY OTHER PERSON OR CORPORATION, OR CONVEYING ANY RIGHTS OR PERMISSION TO MANUFACTURE, USE OR SELL ANY PATENTED INVENTION THAT MAY IN ANY WAY BE RELATED THERETO.

Reproduced by  
**DOCUMENT SERVICE CENTER**  
KNOTT BUILDING, DAYTON, 2, OHIO

# UNCLASSIFIED

AD NO. 40814

ASTIA FILE COPY

ELASTIC SCATTERING OF 20.6-MEV PROTONS BY DEUTERONS

David O. Caldwell\*  
J. Reginald Richardson

Technical Report No. 22

Project Designation Number NRO22-053

Contract N6onr-275 Task Order IV

Under the Joint Program of the  
Office of Naval Research and the  
Atomic Energy Commission

Department of Physics  
University of California  
Los Angeles, California

July 1954

\*Assisted by Atomic Energy Commission Predoctoral  
Fellowships and a National Science Foundation Postdoctoral  
Fellowship

### Acknowledgments

Beneficial discussions were had with Profs. Gregory Breit, Egon Bretscher, K. R. MacKenzie, H. S. W. Massey, and Byron Wright, and Prof. C. L. Critchfield generously supplied the second-order geometry correction. George Jones and Harry E. Handler furnished considerable aid with the electronics, as did Steve Plunkett in the design and construction of the other apparatus. Help in this construction was also given by the personnel of the Physics Department Shop, under the supervision of E. M. Griffiths. Herbert N. Royden's work on the electrometer and its calibration is gratefully acknowledged, as is the extensive assistance given by Miriam Caldwell in the mathematical and computational tasks. One of us (D.O.C.) wishes also to thank Prof. P. Scherrer for the hospitality of the Physics Institute of the Swiss Federal Institute of Technology during the period when much of this report was written.



## ABSTRACT

The absolute differential cross section for the elastic scattering of 20.6-Mev protons by deuterons was measured, using the external beam of the U.C.L.A. synchrocyclotron. A triple-coincidence proportional counter telescope, with variable absorbers between the second and third counters and differential pulse-height discriminators (set by a new method) on the first two counters, was used to select the desired particle by range and specific ionization. Deuterium gas at atmospheric pressure provided the target for the proton beam, which was collimated to  $1/8''$  diameter, with a maximum angular divergence of  $\frac{1}{2}^\circ$ . An interchangeable slit system was used to give angular resolutions of  $0.9^\circ$  or  $1.8^\circ$ . Absolute measurements were made at 22 angles from  $12^\circ$  to  $164^\circ$  (center of mass) with an accuracy varying approximately from 1% to 3%, depending upon the angle. The cross section shows the familiar deep minimum (near  $130^\circ$  in the present case), but in addition a shallower minimum near  $18^\circ$ , due to Coulomb-nuclear interference. This latter minimum should allow fitting the data with a unique set of phase shifts. Heretofore such three-body scattering experiments have by themselves yielded two ambiguous sets of phase shifts, corresponding to the ambiguity in the doublet and quartet scattering lengths. This experiment, then, ought to provide a more stringent test for theories than previous low or intermediate energy nucleon-deuteron scatterings.

## TABLE OF CONTENTS

<u>Chapter</u>	<u>Page</u>
I. INTRODUCTION . . . . .	1
A. Previous work in the field . . . . .	1
B. Charge symmetry of nuclear forces . . . . .	1
C. Exchange nature of nuclear forces . . . . .	3
D. Existence and nature of a three-body force . . . . .	4
II. EXPERIMENTAL METHOD . . . . .	6
A. Requirements imposed for checking on theory . . . . .	6
B. Geometrical limitations and arrangement . . . . .	7
C. Telescope vs. conjugate counter systems . . . . .	7
D. Separation of particle groups . . . . .	8
III. DETAILS OF THE APPARATUS . . . . .	10
A. Cyclotron . . . . .	10
B. Chamber . . . . .	10
C. Collimator . . . . .	11
D. Analyzing slits . . . . .	13
E. Absorbers . . . . .	17
F. Counters . . . . .	19
G. Electronics . . . . .	21
H. Current integration . . . . .	24
I. Vacuum system . . . . .	31
J. Deuterium system . . . . .	32
IV. PROCEDURE AND EXPERIMENTAL CHECKS . . . . .	35
A. Run procedure . . . . .	35
B. Check runs . . . . .	37
V. RESULTS . . . . .	42
A. Corrections to the data . . . . .	42
B. Summary of errors . . . . .	44
C. Beam energy determination . . . . .	47
D. Conclusions . . . . .	49
BIBLIOGRAPHY . . . . .	51
APPENDIX . . . . .	57
FIGURES . . . . .	61

## LIST OF TABLES

<u>Table</u>	<u>Page</u>
I. Fraction of the Deuteron Beyond the Impact Parameter for Various Energies . . . . .	4
II. Dimensions of the Analyzing Slits . . . . .	14
III. Constants of the Slit Geometry . . . . .	15
IV. Experimental Data . . . . .	50

## LIST OF FIGURES

<u>Figure</u>	<u>Page</u>
1. Laboratory Angles vs. Center of Mass Angle . .	61
2. Particle Energy vs. Laboratory Angle . . . . .	62
3. Sectional View of the Scattering Chamber . . . .	63
4. Energy Loss Distribution in a Counter vs. Proton and Deuteron Energy . . . . .	64
5. Electronics Block Diagram . . . . .	65
6. Differential Cross Section for 20.6-Mev P-D Elastic Scattering . . . . .	66

## I. INTRODUCTION

The study of the scattering of nucleons by deuterons could be expected to yield information on (1) the character of the force between neutrons, as compared with that between protons; (2) the exchange properties of nuclear forces; and (3) the existence and nature of three-body forces.

Because of the importance of these subjects, a considerable amount of work has already been done in this field. For example, at least some information is available on the differential cross section for proton-deuteron elastic scattering at the following proton laboratory energies (in Mev): .2 to .9,<sup>1\*</sup> .250,<sup>2</sup> .275,<sup>2</sup> .48,<sup>3</sup> .60,<sup>3</sup> .73,<sup>3</sup> .825,<sup>4</sup> .830,<sup>5</sup> .99,<sup>3</sup> 1.11,<sup>3</sup> 1.23,<sup>3</sup> 1.36,<sup>3</sup> 1.50,<sup>3</sup> 1.51,<sup>4</sup> 1.61,<sup>3</sup> 2.08,<sup>4</sup> 2.53,<sup>4</sup> 3.00,<sup>4</sup> 3.35,<sup>6</sup> 3.49,<sup>4</sup> 3.97,<sup>7</sup> 4.2,<sup>6</sup> 4.97,<sup>8</sup> 5.0,<sup>9</sup> 5.1,<sup>10</sup> 5.2,<sup>11</sup> 9.7,<sup>12</sup> 31,<sup>13</sup> 95,<sup>14-16</sup> 112,<sup>16</sup> 138,<sup>16</sup> 146,<sup>17</sup> 240,<sup>18</sup> and 345.<sup>19</sup> The angular distribution of neutrons scattered from deuterons has also been investigated at a large number of energies:  $7.24 \times 10^{-8}$ ,<sup>20</sup> .135,<sup>21</sup> .220,<sup>22</sup> .280,<sup>21</sup> .446,<sup>21</sup> .500,<sup>22</sup> .588,<sup>21</sup> .750,<sup>22</sup> .780,<sup>21</sup> .914,<sup>21</sup> 1.0,<sup>22</sup> 1.35-1.50,<sup>23</sup> 1.50,<sup>22</sup> 2.0,<sup>22</sup> 2.5,<sup>22</sup> 2.53,<sup>24</sup> 2.6,<sup>26</sup> 2.6-3.1,<sup>27</sup> 3,<sup>28</sup> 3.1,<sup>29</sup> 3.27,30,<sup>31</sup> 4-6,<sup>27</sup> 4.5,<sup>32</sup> 5.5,<sup>32</sup> 6-9,<sup>27</sup> 9.7,<sup>33</sup> 12-13,<sup>34</sup> 13.9,<sup>33</sup> 14,<sup>35</sup> 36 and 90<sup>37</sup> Mev (neutron laboratory energy). While the inelastic scattering has received much less attention, a little information on the  $D(p,2p)N$  reaction is available at proton laboratory energies of 5.1,<sup>38</sup> 9.7,<sup>39</sup> 95,<sup>14</sup> 40,<sup>41</sup> 240,<sup>16</sup> and 340<sup>42</sup> Mev, and on the  $D(n,2n)P$  reaction at neutron laboratory energies of 12-13,<sup>34</sup> 14,<sup>35</sup> 36,<sup>43</sup> 90,<sup>37</sup> and 270<sup>44</sup> Mev.

There has also been a large quantity of theoretical work done in this field. The early papers,<sup>45-49</sup> those<sup>50-53</sup> dealing only with methods of making three-body calculations, the work<sup>54-57</sup> on very low energies, and that<sup>58-71</sup> utilizing Born or "impulse" approximations (i.e., for energies above 80 Mev) will not be of interest with regard to the present experiment. We are concerned with the intermediate energy region, for which theoretical work has been done on  $n$ - $d$ <sup>72-76</sup> and  $p$ - $d$ <sup>77-84</sup> (often with  $n$ - $d$  included) elastic and inelastic<sup>85-87</sup> scattering.

Let us see what can be concluded from all this work in regard to the first objective mentioned above, determining whether charge symmetry exists; i.e., whether the forces between two neutrons are the same as those between two protons, aside from Coulomb and mass-difference effects. Since neutron-neutron scattering is impracticable, the next most direct way to get information on the  $n$ - $n$  force would seem to be by comparing  $n$ - $d$  and  $p$ - $d$  scattering, as the  $n$ - $n$  force involved in one is replaced by a  $p$ - $p$  force in the other. Comparing differential cross sections - or, a much better test, comparing similar phase shifts - for  $n$ - $d$  and  $p$ - $d$  scattering

---

\* References are collected at the end.

up to 5 Mev has given evidence <sup>22, 80, 81, 83</sup> for charge symmetry. The p-d phase shifts seem to be less than the corresponding n-d ones by the square of the Coulomb barrier penetrability factor.<sup>80</sup> Looking at it another way, the p-d phase shifts are essentially equal to those for n-d if the proton laboratory energy is higher than that for the neutron by 0.5 Mev, the height of the Coulomb barrier.<sup>83</sup>

This evidence for charge symmetry is not very decisive, however, because of the inaccuracy of the n-d experiments used for comparison. It seems worthwhile to make better experimental comparisons in this intermediate energy region, where the charge symmetry assumption can be tested for several angular momentum states, and where the most accurate n-d experiments can be done, using monoenergetic neutrons from the  $T(d,n)He^4$  reaction. Such experiments have been performed at 14 Mev<sup>35, 36</sup> and others are expected to be done at 27 Mev,<sup>88</sup> but an ideal comparison with the present p-d experiment could be provided by using the 20-Mev neutrons available from the new Los Alamos electrostatic generator.

The recent calculations of Christian and Gammel<sup>84</sup> seem to show that a comparison of only quite accurate n-d and p-d experiments could yield much information on the n-n force. They find that the n-n and p-p forces are relatively unimportant in nucleon-deuteron scattering, the phase shifts being determined mainly by the triplet even parity n-p force. This result may stem largely from their choice of slow-neutron scattering lengths on which to base phase shifts, whereas another set of scattering lengths is also allowed by experiments.<sup>89</sup>

It is an important characteristic of the nucleon-deuteron scattering work reported so far that each experiment could be fitted by two sets of phase shifts, corresponding to the ambiguity in the scattering lengths. While such an indeterminateness is inherent in n-d scattering (unless the experiment could be performed with polarized neutrons) a unique set of phase shifts would be obtainable from p-d scattering, if the region of interference between Coulomb and nuclear forces were accurately observed. So far p-d experiments have either not been extended to low enough angles, or have been too inaccurate at low angles to provide the needed additional condition which would remove this ambiguity.

Thus it would seem that p-d and n-d experiments more adequate than those heretofore compared are needed to provide a test of the charge symmetry hypothesis, or even to establish which set of phase shifts is the correct one. A similar conclusion can be reached for the second aim, mentioned at the beginning of this section, that of determining the exchange character of nuclear forces. While nucleon-deuteron scattering has fairly well established the existence of exchange forces, as opposed to ordinary forces, the more difficult distinction

among types of exchange forces will require more complete experimental and, particularly, theoretical work.

Nucleon-deuteron scattering can provide information on the exchange nature of nuclear forces because the deuteron is loosely bound and thus makes a relatively big target, so that even fairly low energy nucleons are scattered in states of angular momentum greater than zero. Similar angular momentum states, which should show the exchange character of the forces, appear in nucleon-nucleon scattering only at much higher energies, where added complications, such as relativistic effects, velocity dependent forces, and possibly isobaric states, enter in to confuse the interpretation of the results.

Three main theoretical approaches are available for attempting to distinguish among force types by comparison with intermediate energy nucleon-deuteron scatterings, that of Massey and his co-workers,<sup>72, 73, 76, 78, 82</sup> that of Verde<sup>74</sup> (applied to p-d for partial waves of  $L > 0$  by Gammel<sup>80</sup>), and that of Christian and Gammel.<sup>84</sup> So far two of the three seem capable of fitting the low energy data fairly well, while the third (Verde's) has not yet been compared with experiment, it being for 20 Mev. The present experiment could provide the first comparison with all three methods.

However, it is too much to expect of the theories that a comparison of this experiment with any of them will provide a definite answer as to the type of exchange force present. The available calculations do not include inelastic scattering, polarization, and tensor forces, nor do the potentials used give satisfactory answers for intermediate energy nucleon-nucleon scattering. More important yet may be the omission of many-body forces.

Since no calculation yet includes the effects of many-body forces, it is perhaps premature to include seeking information about such forces as the third possible purpose for investigating nucleon-deuteron scattering. However, the recent work of Drell and Huang<sup>90</sup> raises the hope that such calculations can be made soon. Generalizing the Lévy<sup>91</sup> two-body potential for many-body forces, they calculated the total energy per nucleon as a function of nuclear density, and found an energy minimum of about the right value at a reasonable nuclear density. Not only could this provide an answer to the long-standing problem of nuclear saturation, but also the introduction of such many-body forces brings into closer accord the successful independent-particle model of the nucleus and meson theories of nuclear forces. The marked position correlation between nucleons resulting from strong, short-range, two-body forces is weakened by the many-body interactions, giving a more smeared-out picture of the nucleus, like that required by the shell model.

The apparent success of the work of Drell and Huang has been achieved without introducing any new parameters in the Lévy potential.

While its field-theoretic basis is now dubious,<sup>90, 92</sup> the potential does fit<sup>91, 93</sup> the data up to 40 Mev for the n-p and p-p systems, while having only two adjustable constants, which are fixed by the binding energy of the deuteron and the n-p triplet scattering length. The generalization of the potential has been carried as far as five-body forces, but the alternating series (even-body forces are attractive and odd-body forces, repulsive) converges so rapidly, due mainly to the Pauli exclusion principle, that only the three-body force is important.

If these calculations represent the true state of affairs,<sup>\*</sup> it seems likely that the repulsive three-body force, which would be almost entirely responsible for keeping nuclei from collapsing, should show up in nucleon-deuteron scattering. A possible indication of its presence might be the appearance of anisotropy in n-d scattering even at an energy as low as .135 Mev.<sup>21</sup> Perhaps at higher energies the effects of a three-body force have been masked by employing so many partial wave parameters in fitting inadequate data.

In line with this conjecture, it is interesting to see that the fraction of the deuteron which could give rise to such high angular momentum values,  $L$ , is very small indeed. Since the best fits to the data obtained so far have been made by Christian and Gammel,<sup>84</sup> the largest  $L$  values they found necessary to use at three nucleon laboratory energies,  $E$ , are listed in Table I, along with the fraction of the deuteron which is found at distances greater than the impact parameter,  $r$ , needed to give these large  $L$  values. This fraction of the deuteron is obtained, using an asymptotic form of the deuteron wave function, from  $\exp[-2(r/\lambda_D)] = \exp[-2L(\lambda_N/\lambda_D)]$ , where  $\lambda_N$  is the nucleon wavelength and  $\lambda_D$  is the deuteron wavelength, as given by its binding energy. In connection with the following table, it should be recalled that although the values of the high angular momentum phase shifts are small, they are quite important to the shape of the differential cross section, since their contribution is weighted by roughly the square of the factor  $(2L + 1)$ .

Table I

$L$	$E$ Mev	Impact Parameter, $r$	Fraction of Deuteron Beyond $r$
6	9.66	$13.2 \times 10^{-13}$ cm.	.0022
4	2.53	$17.2 \times 10^{-13}$ cm.	.00035
4	1.51	$22.2 \times 10^{-13}$ cm.	.00003

While little more than guesswork is possible now, if it is practicable to work out nucleon-deuteron scattering using something like a generalized Levy potential, a comparison of phase shifts from such a theory with phase shifts from the present experiment, for which the

\* Somewhat similar results are obtained by Wentzel,<sup>94</sup> using scalar pair theory.

kinetic energy is much like that within a nucleus, might yield interesting information on the role of many-body forces inside nuclei.



## II. EXPERIMENTAL METHOD

From the preceding discussion, we have seen that it is highly desirable in measuring the angular distribution of protons scattered from deuterons to carry the measurement down to low angles in order to cover the region of Coulomb-nuclear interference. Since the scattering will be almost purely Coulomb, and therefore not very interesting, at too low an angle, we note that the maximum angle at which Coulomb scattering is important is given roughly by the square root of the ratio of the barrier energy to the kinetic energy.<sup>\*</sup> At 20 Mev this angle is  $90^\circ$ . To be safe, the apparatus was designed to work down to  $8^\circ$ , which for protons corresponds to a center of mass angle of  $12^\circ$  (see Fig. 1; all figures are collected at the end).

It is desirable to include not only the very low angles, but also the very high ones, because the theoretical results so far obtained differ mostly in the relative sizes of the forward and backward peaks, and to a lesser extent in the position of the minimum. Thus we wish to measure as close as possible to a center of mass angle of  $180^\circ$  (or, from Fig. 1, also a laboratory angle of  $180^\circ$ ), but from Fig. 2 we see that the proton energy at this angle is 2.3 Mev. Because multiple scattering losses increase rapidly as the energy decreases, it is not desirable to count back-scattered protons. Instead, we count the recoil deuteron which goes forward with most of the energy. From Fig. 1 we see that counting deuterons at the limiting angle of  $8^\circ$  corresponds to a proton center of mass angle of  $164^\circ$ .

Paranthetically, it should be noted that the formulas necessary for computing the curves of Figures 1 and 2 may be found in the Appendix. Classical and relativistic formulas are given for both the laboratory vs. center of mass angles and energy vs. laboratory angle relations. While the difference between the classical and relativistic results is small, relativistic expressions were used for transforming both the laboratory angles and cross sections to the center of mass system (cf. Appendix).

Trying to achieve the minimum angle of  $8^\circ$  required some compromises because a large scattering chamber was impracticable, since the target gas, deuterium, is expensive. Also, since the gas ought to be purified by passing it through a heated Pd tube, the filling time is slow, further militating against a large chamber. A small chamber, of inside diameter slightly less than 11", was available, and this, then, provided the main limitation on the geometry.

---

<sup>\*</sup> The maximum sidewise momentum which the proton can acquire in such a collision is proportional to the square root of the Coulomb barrier energy.

Let us look at the general geometrical arrangement. The proton beam came into the chamber through a collimating system, which defined it to  $1/8''$  and limited its angular divergence to not more than  $\pm 1/2^\circ$ . A small part of the beam was scattered by the deuterium gas at atmospheric pressure which filled the chamber. The unscattered beam passed through the chamber, an exit foil, and then into an evacuated Faraday cup where the total beam charge was determined for a scattering run. A small part of the scattered beam was selected by a slit system and counted by proportional counters. The slit and counter system was on an arm mounted on a shaft which could be turned from outside the chamber. Also attached to the shaft was a disc on which the scattering angle could be read.

With this description in mind and with the aid of Fig. 3, we can return to the question of the geometrical limitations. In order to keep the corrections for finite angular resolution small and yet to maintain a reasonable counting rate, two interchangeable sets of slits were made, of angular resolution  $\pm 0.9^\circ$  and  $\pm 1.8^\circ$ . The narrow slits were used at small angles, where the counting rates were higher and the cross section changed rapidly with angle, while the wide slits were used at the larger angles (intermediate center of mass angles), where the counting rates were lower and the cross section was flatter. Having interchangeable slit systems was valuable for several experimental checks also, as will be discussed later.

With the minimum angle and the angular resolution chosen, the position of the front slit on the counter arm is essentially determined, since the slit must miss the unscattered beam at the lowest angle. The position of the rear slit requires further consideration. To obtain wide enough slits and to maximize the solid angle for a given angular resolution, it is desirable to push the rear slit as far back on the counter arm as possible, but it was felt necessary to provide room for three counters in triple coincidence, in order to reduce the accidental coincidence rate and to provide better particle selection. In order, then, to have simultaneously a practical slit geometry, a small minimum angle, a good angular resolution, a large solid angle, a triple-coincidence counting system, and a small chamber, it was necessary to resort to the unusual expedient of putting the rear slit between the second and third counters. This means that the windows of the first two counters served as anti-scattering baffles. As will be discussed later, this arrangement imposed stringent limitations to avoid multiple scattering losses between the slits.

A triple-coincidence counter telescope was chosen in place of the other alternative of conjugate coincidence counters, which count both the scattered and recoil particles, for many reasons, a few of which are given here. The conjugate counter system is not good for small angle measurements, because of multiple scattering losses and because the angular resolution gets worse as the angle decreases.

The accidental coincidence rate is higher for the conjugate system because (1) there are two counters instead of three; (2) the conjugate counter must be made large (a) to reduce multiple scattering losses, and (b) because its effective height and width are a function of angle, one varying inversely with the other; and (3) the solid target which must be used will have higher Z constituents. Also, the number of target particles cannot be determined as accurately for a solid target as for the gas one which can be used with the telescope system.

One considers the conjugate counter system in the first place because with the telescope system one must separate five groups of particles: scattered protons, recoil deuterons, protons from the deuteron disintegration. Protons scattered from hydrogen (an impurity in the deuterium), and protons scattered from heavy contaminants, such as air. Since all the information desired in this experiment cannot be obtained with the conjugate counter system, we must separate the particles by their range (with absorbers) or by their energy (with a scintillation counter). While a scintillation counter is not practical in a chamber of this size, separation by range is more desirable in some respects, in any case. For example, at a given angle the range ratio for scattered proton to recoil deuteron is much greater than the corresponding energy ratio. Another advantage is that with absorbers one can separate almost completely (i.e., to 0.1%) two proton groups which differ in energy by only 6%. This not only gives a better separation of the particle groups, but also it makes the corrections for slit-edge penetration much smaller.

There is a continuous distribution in energy of the protons from the break-up of the deuteron, ranging from zero to a maximum energy, which occurs for the case of one proton going off in one direction and the neutron and other proton going off in the opposite direction. This maximum energy is plotted in Fig. 2. To count deuterons, this background proton continuum was discriminated against by using the difference in the proton and deuteron specific ionizations as the particles passed through the first two counters. In order to provide a separation on the basis of specific ionization, and also to reduce the single-counter counting rates, differential pulse-height discriminators were used in the first two counting channels. The absorbers were chosen so that the desired particle was near the end of its range in the third counter; the resulting large pulse was then distinguished with an integral discriminator. In this way deuterons were counted to the exclusion of the longer range protons.

Separating particles by specific ionization at these energies is made difficult by the high probability that a large energy loss will occur in a single collision.<sup>95-100</sup> Computations of this effect have been made on the basis of Symon's<sup>100</sup> rather complete version of the

energy loss theory, and the results are presented in Fig. 4. The energy loss distribution of protons and deuterons in a counter filled with one-half atmosphere argon is given. Curves are drawn for various percentages of a group of monoenergetic particles, and for each percentage the curve gives the maximum energy loss for various proton or deuteron energies. The broadness of this energy loss distribution (represented at a given energy by the difference in energy loss for the 0.1% and 99.9% curves), rather than the resolution of the proportional counters, determined the extent to which particles could be distinguished by this means and made necessary some correction for the background of disintegration protons when counting deuterons.

Having a general idea of the methods chosen for this experiment, we can now go on to the details of the apparatus used to carry it out.

### III. DETAILS OF THE APPARATUS

#### A. Cyclotron

The scattering equipment was used with the U.C.L.A. cyclotron, which has 41" pole-pieces, is frequency-modulated, and by means of an electrostatic deflector produces a 21-Mev proton external beam in 20 microsecond bursts, 1000 times a second.

The external beam was made approximately parallel in the vicinity of the scattering chamber by means of a double-focusing wedge magnet in the cyclotron field. Coming out between 18" thick water walls through a magnetically shielded pipe, the beam passed into the scattering chamber collimator, which was attached to the pipe by a flange and sylphon. The chamber itself was approximately 10 feet from the cyclotron tank. The water walls and some additional paraffin provided neutron shielding, but it was found that the main neutron and gamma background came from the external, rather than the internal, beam. This background was reduced greatly by letting nearly all the external beam strike only carbon (which has a high threshold for neutron production), both in the collimator and in the Faraday cup.

#### B. Scattering chamber

The chamber itself, a brass casting of 10-29/32" inside diameter and 3-1/8" inside height, has been used previously in conjugate-counter scattering experiments.<sup>101, 102</sup>

In order to be more sure of the chamber alignment, the exit (Faraday cup) and entrance (collimator) holes were rebored. This was done by putting through the central hole in the bottom of the chamber a tight-fitting plug, which was placed in the jaws of a rotary table. The bottom inside of the chamber and the top lip of the chamber were both checked with a dial indicator and found to be properly level. With the rotary table at 0°, the entrance hole was rebored and the face on which the collimator flange rested was milled off perpendicular to the bore. The same procedure was repeated at the exit hole with the rotary table turned to 180°. An O-ring groove was put in the central hole in the chamber, but the same ground brass shaft, which was previously used just with a grease seal for vacuum tightness, was again used in this hole to support the arm on which the slit system and counters turned. Thus this shaft and the hole into which it was rather tightly fitted provided the reference for aligning the geometry of the whole system.

To aid in the later final alignment of the system, a steel pin was placed in the center of the shaft, so as to project a

short distance into the chamber. The shaft was held in place on one end by a ball bearing assembly which bore against the outside bottom of the chamber and on the other end by a tight-fitting cap, which was screwed to the top of the shaft. Attached to the bearing assembly was a 10" diameter graduated disc, on which the counter angle could be read. On the other end of the shaft, the counter arm was bored out to fit tightly on the cap. The whole counter turning and indicating system -- arm, cap, shaft, bearing assembly, and graduated disc -- was put together with steel dowel pins, so that it could be disassembled and then all its parts returned, quite accurately, to their previous relative positions.

### C. Collimator

The collimator construction is best explained by referring to Fig. 3. Originally it was made to utilize the supposedly accurately bored hole in the chamber for alignment. Thus the part of the collimator extending into the chamber made a tight fit in this hole, while the external tube of the collimator fitted tightly on the inner tube. However, a slight inaccuracy in the bore made it necessary to provide set-screw adjustments on the second defining hole and the last anti-scattering hole.

The edges of the brass defining diaphragms were  $1/32$ " thick, the first hole being .1248" in diameter and the second, .1236". Their defining edges were 14.22" apart, giving a maximum angular divergence of the beam in the chamber of  $\pm 0.50$  degrees.\* This geometry gave a reasonable beam strength, and yet the correction to the cross section for finite beam size was small.

All non-defining diaphragms were made of carbon to reduce both the scattering and the neutron background, as was explained previously. To further reduce scattering, these diaphragm edges were beveled. Most of the unused external beam was stopped by a carbon insert in the flange which joined the collimator to the cyclotron, and most of the rest on an insert just ahead of the first defining hole. Between the two defining holes were three non-defining holes spaced by aluminum sleeves so that the following criteria were fulfilled: (1) the most divergent incident proton would not see the collimator wall; (2) no part of the collimator wall could see the last defining hole (except for the section adjacent to that hole); (3) protons scattered off the first defining hole would not see the collimator wall (except for the first section); and (4) no part of the collimator wall could see the Faraday cup entrance. These criteria made the collimator effectively wall-less. A final anti-scattering hole of .170" diameter was added 1.790" beyond the second defining hole to limit the spray of protons off the last defining hole edge to a cone of half-angle  $4.7^\circ$ .

---

\* Actually, the part of the beam selected by the collimator was so nearly parallel that beam pictures showed essentially all the beam to be contained within an angular divergence of  $\pm 0.2^\circ$ .

The collimator extended as far as possible into the chamber consistent with not entering the scattering volume, the second defining hole being 2.841" from the chamber center. This served two purposes: (1) to keep the beam area small, in order both to make low angle measurements possible and also to permit a small Faraday cup opening; and (2) to reduce the penetration of the first slit of the counter slit system by low-angle protons.

Magnetic shields were provided around both the inner and outer collimator sections. However, it was found that the iron water walls made a more than adequate shield against the cyclotron's magnetic field, and the inner shield was removed.

The foil which separated the cyclotron vacuum from the chamber was just ahead of the first defining hole. In order to keep small the loss of beam from multiple scattering, .0005" mylar (a DuPont polyester) film was used. At first, .001" nylon was employed, but it developed leaks under bombardment much more rapidly than did the mylar.

As mentioned previously, some alignment of the collimator was necessary to be sure that the beam (1) passed through the central axis of the chamber, (2) was perpendicular to that axis (i.e., parallel to the plane of rotation of the counters), (3) was at the same height as the midpoint of the counter slit system, and (4) lay along the  $0^\circ$ - $180^\circ$  direction. In order to locate the chamber center, a .014"-diameter steel needle was attached by a set-screw arrangement to the previously described steel pin in the center of the shaft on which the counters turned. The centering of the steel needle was checked to better than .002" by looking at its flat top with a traveling microscope while rotating the counter shaft. The height of the needle was set to within .002" by using a dial indicator and an accurately milled and measured block placed on the counter arm in the same position as gauge blocks had previously been put to set the heights of the counter slits.

Most of the alignment was done by looking through the collimator with a transit. With the second defining diaphragm removed, the transit was set so that its cross-hairs could be centered on the first defining hole and the centering needle. The set screws on the last anti-scattering hole were adjusted to center that hole on the cross-hairs; then it was removed, the second defining diaphragm inserted, and the anti-scattering hole returned to its original setting. The second defining hole was centered next. With the transit thus coincident with the collimator axis, the difference in heights of the centering needle and the milled block on the counter arm was found to be less than .003". This corresponds to a maximum angle between the collimator axis and the plane of the counter rotation of  $.08^\circ$ , giving negligible errors in the scattering cross section ( $10^{-4}\%$ ) and the counter angle ( $.0004^\circ$ ).



Also with the transit so aligned the zero position of the counter-angle disc was set. The first step was to set the counter arm so that the first counter slit was centered on the centering needle. A slight adjustment was then made to take care of the known (to be discussed later) small distance by which the axis of the counter slit system missed the central axis of the chamber. The total error in the counter angle measurement introduced by these two adjustments is  $.04^\circ$ .

Since an appreciable error could occur in the small-angle scattering measurements if the beam did not pass through the center of the chamber, the final check on the adjustment of the second defining hole in the collimator was made with the proton beam itself. With the chamber evacuated, photographic paper placed directly behind the centering needle was exposed to the beam. By measuring with a traveling microscope the position of the needle shadow with respect to the beam circle, the beam centering could be checked to within  $.002''$ . This, combined with the error in centering the needle, gives an error in the cross section of less than  $.0649\%/\sin\theta_0$ , where  $\theta_0$  is the counter angle. Thus the error varies from  $0.46\%$  at  $8^\circ$  to  $0.06\%$  at  $90^\circ$ , and is essentially zero for an average of two measurements made at equal  $\theta_0$ 's on both sides of the beam. A further error due to the beam's shifting will be discussed later.

#### D. Analyzing slits

It has already been explained that there were two interchangeable sets of analyzing, or counter, slits (of  $\pm 0.921^\circ$  and  $\pm 1.800^\circ$  angular resolution), and that the slit system was on the counter arm, which turned on a shaft through a hole in the chamber center. The reasons for locating the second analyzing slit between the second and third counters have also been discussed. Here we shall be more concerned with the method of making and measuring the slits and the resulting errors in the geometry.

The material chosen for the slits was commercial bronze, as a compromise between workability and high copper content (90% Cu and 10% Zn). Copper is a good material for slits, since it has a relatively high density with a relatively low Z, desirable features for reducing slit-edge penetration. To further reduce such penetration, the region of each slit plate around the slit opening was milled down to  $.030''$ , a stopping thickness for 20-Mev protons.

Because each of the four slits was made in one piece, each had to be hand filed after the initial milling. Short periods of filing were interspersed with long periods of slit measuring, using a traveling microscope. This tedious process was continued until each slit opening had quite uniform edges and both sets of slits were accurately interchangeable. It was also desirable to make the front and rear slits of each set of the same width, since this maximizes the solid angle for a given angular resolution and also reduces the second-order geometry corrections.



The slit dimensions were measured using a Gaertner #1065 Traveling Microscope, fitted with a Leitz Ultropak illuminating objective, giving a total magnification of 65x and permitting illumination of the slit from above and below, to aid in distinguishing the slit edges. While the microscope read directly to .0001", with .00001" easily estimated, it was necessary to calibrate the microscope with gauge blocks to achieve this accuracy. This calibration gave a correction of about 0.1%.

The solid-angle-scattering-length product seen by the third counter is defined by the height (H) and width ( $D_R$ ) of the rear slit, its distance from the scattering center ( $r_2$ ), the width of the front slit ( $D_F$ ), and the distance between the slits ( $r_1$ ), and is given by

$$\int \omega dl = HD_F D_R \sin \theta_0 / (r_1 r_2) = \frac{\sin \theta_0}{G},$$

where  $\theta_0$  is the counter angle. In order to measure accurately the area of the rear slits and the width of the front slits over only that portion which is effective in limiting the scattered beam, use was made of the bidirectional travel of the microscope to provide a grid. As an example, when finding the narrow rear slit's width, measurements were made at intervals of .025" along the slit's length. Five series of such measurements were made, each series starting .005" from the previous one. Thus, the width was measured every .005" along the length. A standard deviation was computed by comparing the averages of each of the five series. This gave an upper limit to the error of the measurement, since some of the differences among the series were due to slit non-uniformity. The results are summarized in the following table, in which the slit heights and widths and the standard deviations of the measurements are all given in inches. The number of measurements made of each dimension is given, and the two sets of slits are classed as "narrow" ( $\pm 0.9^\circ$ ) and "wide" ( $\pm 1.8^\circ$ ).

Table II

Slit	Width	Std.Dev.	No. of Meas.	Height	Std.Dev.	No. of Meas.
Front Narrow	.051552 $\pm$	.000059"	112			
Rear Narrow	.052269 $\pm$	.000075"	119	.59234 $\pm$	.00016"	51
Front Wide	.101023 $\pm$	.000041"	56			
Rear Wide	.101879 $\pm$	.000044"	60	.59249 $\pm$	.00010"	51

Since the two sets of slits slid into their holders, it was necessary to make the distances from each slit center to the edges of the slit plate accurately the same for both sets. Knowing these distances to about .0001" made possible the accurate alignment of the slits and their holders by means of dial indicators. To facilitate the alignment procedure, the entire counter arm was made removable and replaceable. As previously mentioned, the arm was partially bored out to fit tightly over a cap which in turn snugly fitted the shaft through the bottom of the chamber. The rotation position was fixed by a dowel pin. This arrangement permitted the counter arm to be set up on a dummy shaft, fitted with an accurately turned center-indicating pin.

Using this arrangement, the slit alignment could be checked and the distances from the scattering center to the last slit ( $r_2$ ) and between the slits ( $r_1$ ) could be measured using both traveling microscopes and indicators with gauge blocks. In all, 8 different sets of measurements were made of  $r_2$  and 10 of  $r_1$ . Of these, the most accurate checks and measurements were made in the Standards Laboratory of the U.C.L.A. Engineering Department, using a Pratt and Whitney ElectroLimit Gage, which read directly to .00005", and Johansson Precision Gage Blocks. A weighted average of the various determinations, in inches, appears in the following table, along with the constant part of the solid-angle-scattering-length factor.

Table III

Slits	$r_1$	Std. Dev.	$r_2$	Std. Dev.	$\frac{H D_F D_R}{r_1 r_2}$ $\frac{\text{cm.}}{\text{sterad.}}$	Per Cent Std. Dev.
Narrow	3.2289 $\pm$	.0011"	4.3895 $\pm$	.0004"	$2.8604 \times 10^{-4}$	$\pm 0.19\%$
Wide	3.2284 $\pm$	.0011"	4.3885 $\pm$	.0004"	$1.09325 \times 10^{-3}$	$\pm 0.047\%$

The accuracy of the slit alignment was checked, and the effect of alignment errors on  $H D_F D_R / (r_1 r_2)$  were investigated for the following slit characteristics: height, left-right positioning, lengthwise and sidewise tilting, rotation, and slit edge non-uniformity. The total errors amount to .004% for the narrow slits and .002% for the wide. The left-right positioning, rotation, and slit non-uniformity contributed to errors in the scattering angle also, and these are .036° for the narrow slits and .042° for the wide.

As has been mentioned when discussing the collimator alignment, a line through the slit axis did not quite pass through the chamber center. However, the amount of the discrepancy (about .003") was accurately measured and could be allowed for in setting the counter angle zero. When the error for setting the zero and that for setting the counters at any desired angle are added quadratically to the slit geometry errors mentioned above, the resulting error in the angle

is  $.063^\circ$  for the narrow slits and  $.065^\circ$  for the wide slits. This angular uncertainty at most angles contributed the largest error in the cross section attributable to the geometry. The error arises mainly from the appearance of  $\sin\theta_0$  in the solid angle factor (cf. p. 14) but also from the angle-dependent part of the center of mass transformation (see the Appendix). The relative error in the cross section is  $\Delta\sigma/\sigma = 2\Delta\theta_0/\sin 2\theta_0$  for deuterons and

$$\Delta\sigma/\sigma = \left[ (\cos\theta + \theta_0) + \sin\theta(3.5 + \cos\theta)/(2 + \cos\theta)^2 \right] \Delta\theta_0$$

for protons (where  $\sigma$  is the cross section,  $\theta$  the center of mass angle, and  $\theta_0$  the laboratory angle). This error varies from 0.13% to as much as 0.79% at  $\theta_0 = 8^\circ$ .

The anti-scattering baffle (B in Fig. 3) attached by dowel pins to each front slit plate was aligned and checked in the same way as the slits. One purpose of the baffle was to reduce slit-edge penetration by preventing particles which scattered off the gas at a smaller angle than those being counted from hitting the front slit. A more important purpose of the baffle was helping to prevent protons scattered off the last defining slit of the collimator from getting into the analyzing slit system. At counter angles of  $15^\circ$  and larger, the last anti-scattering hole on the collimator also prevented direct slit-slit scattering, but between  $15^\circ$  and  $10^\circ$  the baffle alone was effective. At  $8^\circ$  direct slit-scattered protons could get through the front analyzing slit, but not past further anti-scattering slits which were placed between the front analyzing slit and the first counter window.

As will be discussed later, protons which underwent more than two scatterings (one of which might be the gas) did get into the first two counters, but these either did not get through the second analyzing slit, or they could not get through the absorber in front of the third counter, because they had lost too much energy in the many scatterings. Such repeated scatterings from metal were bothersome only at the very small angles and then only because of the increase in the single-counter counting rates in the first two counters. These rates were reduced by stopping down the first counter window opening with a Lucite insert when the narrow slits were used.

The anti-scattering baffle was effective only when the counters were on one side of the beam, but the action of the baffle was important only at small angles, and it was necessary to take all the small-angle data on that side of the beam, anyway. Measurements could not be made on both sides of the beam below  $45^\circ$ . This unfortunate limitation was another compromise which had to be made in order to get down to  $8^\circ$  and still achieve all the features considered necessary for a successful experiment, as has been discussed under "Experimental Method." Thus the front slit and first two counters were made asymmetrically, so that they could be moved close to the unscattered beam on one side. For the same reason, the anti-scattering baffle was placed on the side away from the main beam.

## E. Absorbers

The use of absorbers between the second and third counters to provide particle selection by range has already been discussed. Here we shall consider making, mounting, and using the foils, and particularly choosing and determining the foil thicknesses.

Since it was necessary to change foils without disturbing the deuterium, the foils were mounted on the rim of a wheel which could be turned through a Wilson seal in the center of the chamber lid. The foils, rectangles of aluminum about  $2\frac{1}{4} \times 25/32$ ", were held by strips of neoprene against a curved frame, which was attached to the wheel rim. The frame and "wheel" actually had an arc length of only  $100^\circ$ , since anything bigger would not be useful, because of obstructions such as the collimator. This whole assembly was insulated and left electrically floating because the foils had to pass through rather a small gap between the second and third counters, the out-sides of which were at about -800 volts. Outside the chamber, a pointer attached to the shaft which turned the absorber wheel indicated on a scale the angular position of the absorbers. All parts determining this angular position, including the chamber lid, were held in place by dowel pins.

For convenience, the foils were made  $10^\circ$  wide. Thus a foil load could include up to 10 sets of absorbers, but this number was never used at one time, since it was necessary to leave generous gaps for the main beam to pass through. This  $10^\circ$  width was about the same as that of the whole third counter, so there was no chance that particles could get around the absorbers and into the counter window, which was about  $5^\circ$  wide. By making photographic checks with the beam, it was found that the foils were positioned to an accuracy of better than  $1/2^\circ$ . Although there is no positioning problem vertically, the foil overlapped the window by a large amount in that direction, too.

The foils were made from samples furnished by the Reynolds Metals Co. and the Aluminum Company of America and were 99.4% pure aluminum. Eighteen thicknesses were used, ranging from .00035" to .040". Two stacks composed of at least two foils of each thickness were clamped tightly and milled to the proper dimensions. Samples were taken from various parts of both stacks and measured on a traveling microscope. For a given stack, there was no variation in area with position in the stack, within the measurement accuracy of  $\pm 0.15\%$  (standard deviation). Thus an average area was used for all foils in one stack.

Each foil was weighed individually, however, on a Christian Becker Chainomatic Balance. Weighings were reproducible to 0.1 mg. for the lightest foils and 0.2 mg. for the heaviest, giving errors of less than .02 mg./cm.<sup>2</sup> in the density. Because of the accuracy of the weighings and the area determinations, and because no varia-

tion with stack or position in a stack could be found, the variation in density for foils of the same nominal thickness was taken as a measure of the variations in foil thickness.

In determining the thickness of absorber to be used, a safety factor of three standard deviations of the foil thickness variation was allowed. Much larger allowances had to be made for the angular resolution of the counters (cf. Fig. 2) and for straggling. Since the straggling calculations have already been published,<sup>103</sup> it is sufficient to mention here that an integral range distribution was obtained, permitting one to find the number of mg/cm.<sup>2</sup> of Al which have to be subtracted from the mean range in order that not more than 0.1% of the particles of the desired energy are lost by straggling. Since the mean range used at a given angle was that corresponding to the largest angle (or lowest energy) the counter slit system could see, the particle loss in the absorbers due to straggling was negligible.

Since the particle energy was determined using the absorbers themselves, many possible errors were diminished in finding the proper absorber thickness. These errors include the uncertainties in the mean excitation potential of Al ( $I_{Al}$ ) and in the effective thicknesses of the deuterium, counter gas, and three counter windows through which the scattered beam had to pass. The energy determination was made by counting protons scattered from hydrogen as a function of absorber thickness, each set of counts being normalized to the same beam current. During the course of data-taking, one determination was made at 25° and two at 20°. In all cases the shape of the range curve showed that the absorbers for the p-d scattering were being chosen safely.

Aluminum was used for the absorber material because its range-energy relation is better known in this energy region than is that of any other material. This point and the results of the energy measurements will be discussed later. Another reason for using aluminum is that its low Z reduced multiple scattering losses.

The loss of particles due to multiple scattering in the absorber was negligible mainly because the third counter window was quite large compared with the analyzing slits, the absorber was close to the window, and the window made very thick (about 50 mg./cm.<sup>2</sup>), so that the largest part of the multiple scattering took place in the window itself. Calculations of the multiple scattering loss were made in two independent ways. First, using the results of Rossi and Greisen<sup>104</sup> for the mean square projected multiple scattering angle,

$$\langle \phi^2 \rangle = (Z_1^2 E_s^2 / 2) \int_0^t dt / E^2$$

(for particles of charge Z going through t radiation lengths of a material, and for  $E_s \approx 10.5$  Mev), and inserting for the energy loss in Al,  $-dE/dx = .20/E^{.78}$  Mev/(mg./cm.<sup>2</sup>), we get for protons going through thick Al,

$$\langle \phi^2 \rangle = 4.55 \times 10^{-2} (E_f^{.22} - E_{in}^{.22}),$$

where  $E_{in}$  is the proton (or deuteron) energy in Mev before, and  $E_f$  after, passing through the absorber. The particle loss was found by numerical integration, and, although the formula derived above gives an overestimate of  $\langle \phi^2 \rangle$ , the loss was found to be negligible. As a check, a second calculation was kindly performed by Dr. W. C. Dickinson, using the method of Dickinson and Dodder.<sup>105</sup> He also concluded the loss to be negligible. There were small losses due to nuclear interactions and single scatterings, but these are considered later, among corrections to the data.

#### F. Counters

As has been mentioned previously, the multiple scattering loss between the two analyzing slits had to be considered carefully. The loss at the second slit was due mainly to the first counter window and to a lesser extent to the counter gas; the contributions of the deuterium and the second counter window, which was right next to the slit, were quite small. Multiple scattering calculations were made using several theories, as a check, but the most accurate are those based on the formulas of Scott.<sup>106</sup> It was found that the multiple scattering loss apparently could be made negligible if (1) the first counter window was made of .00025" duraluminum, (2) the counter gas (95% A + 5% CO<sub>2</sub>) was at 1/2 atmosphere, (3) the narrow slits were not used for particles of energy less than about 15 Mev, (4) the wide slits were not used for particles of less than about 7 Mev energy, and (5) the beam at the second slit was much larger than the slit, to provide compensating scattering into the slit opening. Reliable quantitative values for particle loss cannot be obtained for this complicated case, since the incident particles were not traveling parallel paths and since the amount of compensating scattering in is hard to estimate accurately. Thus it was advisable to perform experimental checks to be sure that particle loss was not important. These checks are discussed in another section.

The thicknesses of the first and third counter windows were fixed by multiple scattering considerations, as discussed above. Since the scattered beam size increased rapidly in the vertical direction, and since ample allowance in beam size in both directions had to be made to ensure compensating scattering in at the second slit, the second counter exit window was quite large, and .001" Al was needed. There was no window between the first and second counters, since they were bored out of the same brass block.

Because of this arrangement, it was necessary to be sure that one counter did not affect the other. A polonium alpha source was placed so that the alphas traversed nearly all of the first counter but did not quite enter the second, and it was found that the counting rate in the second counter was just background, while that in the first was several thousand a second. Furthermore, the few counts from the second



counter were not in coincidence with those from the first. On the other hand, when the source was moved closer so that the alphas could get into the second counter, all the counts above background from the second counter were in coincidence with those from the first.

Returning to the limitations placed on the counter system by multiple scattering considerations, we have seen that the pressure of the A-CO<sub>2</sub> filling was limited to about 1/2 atmosphere. This pressure, measured on a Bourdon gauge, was used throughout the experiment. The actual gas mixture used, 95% A + 5% CO<sub>2</sub>, was chosen on the basis of empirical curves,<sup>107</sup> which show that for this mixture the ion drift velocity is a constant for values of  $X/P$  (where  $X$  is the field strength measured in volts/cm. and  $P$  is the gas pressure in mm. Hg) ranging from 0.5 to at least 3.0. Since the counters were operated at an  $X/P$  value of about 2.9, changes of counter voltage or pressure did not change the drift velocity, a desirable feature for fast coincidence work.

The gas mixture was prepared by methods assuring high purity, and the counter system was thoroughly cleaned. When not in use, the counter system was continuously pumped, and a fresh filling was used for each night's run. To further ensure that no electronegative impurities interfered with the counters' operation, no organic materials were present in the counter system when the counters had been filled. The window gaskets were cut from a sheet of indium, .010" thick. This thickness was found to be necessary to obtain a vacuum-tight seal, because of the difficulties of having rectangular windows and having too little room in the small counters to have many screws and heavy frames to hold the windows on. To further eliminate organic materials, joints in the 1/8" copper gas line, which fed all three counters, were made with lead gaskets and revised small commercial compression fittings. The two parts of the fitting squeezed the tiny lead "doughnut" into a seat made up of the copper tubing and a small disc soldered to the tubing.

The filled counters were shut off from a Lucite and O-ring rotary joint by a small valve located close to where the gas line emerged from the chamber through a kovar-glass vacuum seal, which was at the bottom of the rotatable shaft holding the counter arm. The insulated rotary joint served the double purpose of allowing the part of the gas line which passed through the counter-supporting shaft to rotate while the rest of the gas system remained stationary, and of separating the counter high voltage, which was fed in on the rotatable part of the gas line, from the rest of the gas system. The outside of the counters, then, had the high voltage, which was usually around -840 volts. Reasons for putting the high voltage on the counter shell rather than on the central wire are<sup>9, 108</sup> (1) no coupling condenser is required between the central wire and the preamplifier, reducing the noise and chance of breakdown; (2) the effective capacitance of the counter is lower, resulting in bigger and faster-rising pulses; (3) the requirements on the high voltage supply as to corona, A.C. pick-up, and regulation are reduced; (4) the biasing conditions of the first pre-

amplifier tube will not be changed by a coupling condenser's resistance becoming comparable to that of the grid leak resistance (here  $10^8$  ohms); and (5) disturbances produced by high voltage leakage in cables and decoupling condensers are minimized.

In usual operation, with the outside of the counters at somewhat over eight hundred volts, a gas amplification of around a hundred was employed. Gas amplification vs. counter voltage curves were run with alpha particles, and the results were about the same for all three counters and about what one would predict. Although the first two counters were made from one brass block and the third was separate, all three were the coaxial cylinder type with inside diameters of .590" and central wires of .003" diameter. The particles traversed the counters perpendicular to the wires. The first two counters were made with the windows placed asymmetrically for the double purpose of allowing the counter system to get down to low angles on one side, as mentioned previously, and preventing the loss of particles which would occur if the scattered beam could strike the counter wires. The third counter, in which the particles stopped, was placed symmetrically with respect to the scattered beam, enabling its window to be made quite large.

As to supporting the central wire, one has to consider holding the wire straight and concentric (to ensure uniform gas amplification), decreasing end effects (for the same purpose), and limiting the active volume (to decrease unwanted counts). The last two requirements conflict, but the reduction of end effects was aided by using supports having a gradually increasing diameter. The .003" tungsten wire was held on each end by an .018" (O.D.) stainless steel hypodermic needle, most of which was inside an .032" (O.D.) needle, which in turn was mostly inside a tapered brass cylinder. The wire and needles were crimped together and force-fitted into the brass, which was then soldered into a kovar-glass seal which had been turned on a lathe to ensure concentricity. The kovar seal fitted snugly into a recess in the counter, made concentric with the main counter bore. Since both ends of the center electrode were connected to the outside, the wire could be glow'd to remove any irregularities or dust on the wire.

The signal lead was .01" wire, which was brought out from the bottom kovar seal on each counter and passed alternately through glass tubing (when passing through metal) and coaxial cable having 6.3  $\mu\text{f./foot}$  (from Transradio, Ltd., London). Care was taken to have the wires well shielded and to avoid multiple grounds. The capacitance of each counter, its cable, and the connector by which its preamplifier was attached at the bottom of the chamber amounted to only 18  $\mu\text{f.}$  The leakage resistance from the center wire to ground or to the outside of each counter was greater than  $10^{13}$  ohms.

#### G. Electronics

We shall follow the electronics block diagram, Fig. 5, in describing the electronic equipment used, starting at the counters. The electronically regulated variable high voltage supply was the conventional type developed for photomultipliers. Over a 24-hour period it



maintained a voltage constant to within 0.1%, even while connected to the regular A.C. lines. Actually, the supply and all the other equipment were operated from Sorensen line-voltage regulators.

The preamplifiers were a slightly modified version of the Los Alamos Model 150,\* which features two 417-A low-noise, high gain triodes (plus a 6AK5) in a cascade circuit which was especially designed for driving a 90-ohm line. To reduce noise, the tube filaments were supplied by a battery, kept charged by a selenium rectifier trickle-charger. The B<sup>+</sup> supply was a Los Alamos Model 41 electronically regulated supply with some added filtering. All grounds were made at the scattering chamber only.

Each preamplifier was connected to the rest of the electronic equipment, which was in the cyclotron control room, by nearly 100 feet of RG-62/U, 93-ohm coaxial cable. The cable was properly terminated at the linear amplifier, which was the well-known Bell-Jordan<sup>109</sup> type. Because of the temperature sensitivity of the overload diodes, these amplifiers had to be altered somewhat. Despite the changes, temperature instability in this and other equipment made it necessary to collect data at night only. Thermometers were installed near the electronic equipment, and an effort was made to keep the temperature constant within a couple of degrees.

The Bell-Jordan amplifiers provided the main limitation on the speed of the counting system, since these amplifiers gave a rise time of slightly less than 0.4  $\mu$ sec. The preamplifiers showed a rise time of less than 0.2  $\mu$ sec., and the counters were faster than that. To be safe, the pulse length used in the pulse-former of the lower level discriminators was made slightly longer than 0.6  $\mu$ sec. This uniform pulse determined the resolving time of the system. Of course, a variety of pulse lengths were tried to be sure that no coincidences were being lost by having too short a resolving time. The different pulse lengths were obtained by switching shorted delay lines in the discriminators, which were the Los Alamos version of the Harwell type. A pulse from the lower-level discriminator went into an anticoincidence unit where it could be blanked by a pulse from the upper-level discriminator, if the signal from the amplifier was higher than the upper-level setting. Complete blanking was assured by delaying the lower-level pulse and making the upper-level pulse twice as long as the lower one. Usually this differential pulse height discrimination was used only on the first two channels, since the large range of pulse heights which had to be accepted in the third counter made integral (lower level only) discrimination more practical.

Those pulses not blanked in the anticoincidence circuit were fed into three different units. First, the single-channel counting rate was monitored by feeding the pulses into a gating unit and thence into

---

\* The authors wish to thank C. Wilkin Johnstone and Richard J. Watts of the Los Alamos Scientific Laboratory for generously supplying circuits, information, and advice.

scalers. Second, the pulses were fed into a coincidence circuit (designed by C. Wilkin Johnstone) used to determine triple coincidences. Third, the pulses also went into a duplicate coincidence circuit which gave a measure of the accidental coincidences.

The two diode-type coincidence circuits could record coincidences among any of the inputs. This was frequently convenient for checking that the 1-3 or 2-3 doubles rate was the same as the 1-2-3 triples rate. The resolving time of either coincidence unit was determined just by the length of the pulses put in. In usual operation, this was within the limits of  $0.71 \pm .04$   $\mu\text{sec.}$  for either unit. The accidental coincidences were determined by requiring a coincidence between counters 1 and 2 and a delayed coincidence with 3. A 1.5  $\mu\text{sec.}$  delay line delayed the pulses from the third counter so that a real triple coincidence could not be recorded as an accidental one. The reasons for choosing this arrangement for registering accidental coincidences will be discussed in a later section.

The outputs from the real and accidental coincidence circuits and from each of the three channels (as previously mentioned) went through gating units to scalers. The gating units determined whether the scalers were allowed to count the various pulses. Except for the accidental coincidence channel, the first scaling down was done in each counting channel by a decade scaler<sup>110</sup> of 5  $\mu\text{sec.}$  resolving time. This scaler proved extremely reliable, a few tube failures being the only trouble experienced in a period of over half a year. The remaining scaling was done for the singles by Berkeley Scientific Co. (Richmond, Calif.) decade scalers, for the triple coincidence by an Atomic Instrument Co. (Boston, Mass.) scale of 64, and for the whole accidental rate by a slightly modified Tracerlab, Inc. (Boston, Mass.) scale of 4096.

The gating units were controlled by the Master Switch, which in turn was controlled by the Master Pulser and the Brown Recording Potentiometer, which recorded the build-up of charge on the beam-integrating condenser at the input of the electrometer. Two types of control could be obtained: (1) all the scalers could be turned on at the beginning of a selected condenser charging cycle and turned off at the end of the same or another charging cycle, and (2) the scalers could be made to count only during cyclotron beam on-times. Usually both controls were used. The first was achieved by having a mercury tumble switch on the Brown Recorder fall when the voltage across the condenser reached a certain value (usually 94.7 mv.); this tripped a relay in the Master Switch which momentarily shorted out the integrating condenser (by means of a solenoid-activated plunger), recorded a condenser dump, turned the timer on or off, and provided a gate to allow or not allow pulses to reach the scalers. The second control was provided by the Master Pulser,\*

---

\* We are indebted to Louis K. Jensen for designing, building, and maintaining this unit, as well as an excellent pulse generator that received continual use.

which was triggered at a selected point in the cyclotron frequency-modulation cycle and provided a pulse which could be varied not only in height and width, but also in its time relation to the cyclotron beam pulse. This gating pulse, which was chosen to be 60  $\mu$ sec. long, could be adjusted so that the 20  $\mu$ sec. beam pulse appeared at its center. This latter gate reduced the chances of getting spurious counts not initiated by the beam by a factor of roughly 60/1000.

Such spurious counts did have to be guarded against, because of the very high gain of the amplifying system. For example, normal cyclotron operation produced no false counts, but parasitics in the R.F. system or bad sparking in the Dee did cause trouble. Reducing other count-giving disturbances, such as turning on fluorescent lights, was another reason for making runs only at night.

The usual checks were made on the linearity of the electronic system and to be sure that there were not unequal time delays in the three counting channels. The nightly checks on the gain, discriminator linearity, gating pulse setting, and scaler operation will be described later.

#### H. Current integration

We shall consider here the collection of the beam, its integration, and the calibration of the integrator. As can be seen from Fig. 3, after the beam traversed the chamber it passed through a .002" duraluminum foil (which separated the deuterium gas at atmospheric pressure from the high vacuum of the Faraday cup), then went through a magnetic field for suppressing secondary electrons, a grounded guard ring, and finally into the partially enclosed end of the long Faraday cup. The beam was stopped in a carbon disc at the far end of the cup, where another magnetic field "curled up" secondary electrons. With this picture in mind, let us discuss the errors that can occur in the beam collection. Such errors can be caused by (1) ionization in the cup region, (2) leakage in the cup or cable, (3) acquisition or (4) loss of secondary electrons, (5) pick-up and rectification of A.C., (6) collection of ions by the electrical leads outside of the cup, (7) loss of electrons from the exterior of the cup by gamma-ejection, (8) loss of part of the beam, and (9) having a low-energy component of the beam (due to collimator slit penetration) which does not produce countable scattering events.

First, let us determine the amount of ionization which could have occurred within the 9" long cup, which was usually kept at a pressure of less than  $1 \times 10^{-5}$  mm. Hg. Since a 20-Mev proton passing through one centimeter of air at atmospheric pressure will form about  $10^3$  ion pairs, the probability of a proton's forming an ion pair when passing through 9" of air at  $1 \times 10^{-5}/760$  of an atmosphere is  $3 \times 10^{-4}$ . Therefore, the upper limit on the error that could have been caused by ionization is .03%. This is an upper limit because it requires that only one member of the pair be collected, whereas it is quite likely that both or none would have been collected and the charge not affected at all.

Entering into a discussion of the possible effects of leakage is the fact that the electrometer used to integrate the beam was of the 100% feedback type, which maintained the Faraday cup near ground potential. This desirable feature was achieved by putting the output of the electrometer, with reversed polarity, in series with the integrating condenser across the Faraday cup. Thus as voltage began building up across the condenser, an equal and opposite voltage bucked it out, reducing the voltage across the cup essentially to zero. Since the gain of the electrometer was quite high and its zero drift quite small, the cup voltage never got far from zero, and leakage problems were greatly reduced. Actually, for most runs (using a  $0.1 \mu\text{f}$  condenser) the voltage across the cup due to the feedback action varied from zero to .0002 volt, while for a few runs (using a  $.01 \mu\text{f}$  condenser) the maximum voltage was .002 volt. Electrometer zero drift was rarely as high as .001 volt. Since the leakage resistance of the cup system was found to be  $3 \times 10^{14}$  ohms, even at the highest voltage ever found across the cup the leakage current was completely negligible.

Since the integrating system was calibrated by putting into it a known current and determining the time it took for the condenser to charge up to its "dumping" value, leakage losses need be considered only for those parts of the integrating system used when measuring beam current, but not when calibrating. With the cup leakage negligible, we have to consider only the leakage of the cable connecting the cup to the electrometer. Actually, some calibrations were made using this cable, and they agreed with others made without it. This is to be expected because the leakage resistance of the cable was found to be about  $2 \times 10^{13}$  ohms, so the maximum possible leakage current was still less than  $10^{-16}$  amp. The lowest charging current used was always larger than  $10^{-12}$  amp. and was usually about  $10^{-10}$  amp.

As to the effect of acquiring secondary electrons, a great deal of work has been done by various experimenters on this question, and when reasonable precautions have been taken, it always turns out that the effect is unimportant. Let us look at the results of some recent careful work by Yntema and White,<sup>111</sup> and see how the present system, while similar to theirs, should have been even less affected by secondary electrons knocked out of the .002" Al foil which separated the Faraday cup vacuum from the deuterium. In both systems, the Al foil was about the same thickness, theirs being .0015". By varying a potential applied to the cup and finding the amount of charge needed to give a certain number of counts in a counter measuring protons scattered at a fixed angle, they found (for a total of 300,000 counts) that the amount of charge was independent of the cup potential over at least the range +6 to -6 volts, provided (1) a magnetic field of at least 500 gauss was present to make the electron paths approximately circular, and (2) that a grounded guard ring was between the foil and the cup. Despite their nearly circular trajectories, a few of the electrons could still have migrated toward the cup if it were positive with respect to the surroundings, but the grounded guard ring prevented the electrons from being influenced by the field of the cup.

In the present experiment the guard ring was made to fit tightly against the Faraday cup housing, which had an inside diameter of  $1\frac{5}{8}$ ". The opening of the ring was made 0.720", whereas the cup opening was 0.875" (although the cup itself had an inside diameter of 1.250"). The front of the  $1/16$ " thick ring was  $9/16$ " from the Al foil and  $3/8$ " from the cup entrance. Thus the cup was well hidden, mechanically and electrically, from the secondary electrons by the guard ring. The maximum diameter which a secondary electron trajectory could have had in the 1250 gauss field, which was supplied by a magnetron magnet just outside the Faraday cup housing, was only 0.24", so considerable migration would have been necessary before even the guard ring could have been struck. Actually, the guard ring was probably more of a refinement than a necessity in the present experiment, since the cup was held so near ground potential, whereas in the Yntema-White experiment the guard ring was needed, since a mechanical slide-back system was used and the cup voltage could reach 0.5 volt, or roughly three hundred times our maximum voltage.

The charge could be in error not only because foil secondary electrons might be added to the cup, but also because secondaries produced when the proton beam was stopped in the cup could escape. This source of error usually receives far less attention, the conventional remedy being to let the magnetic field for suppressing foil secondaries also try to keep the stopping secondaries from leaving the cup entrance. Indeed, in some experiments the cup is maintained at a high negative potential to repel foil secondaries, but this also provides a good way to lose stopping secondaries. In the present experiment, not only was one magnetic field present at the cup entrance, but also another, of 1900 gauss (provided by another magnetron magnet outside the cup housing), was placed at the far end of the cup, where the beam stopped. In addition, the cup was made much longer (9") than is usual, and its entrance was partially enclosed. By the geometry, then, the escape of secondaries was made more difficult in two ways: (1) there was a very small solid angle for escape, and (2) the secondaries could not be influenced by any potential difference between the cup and the region outside it. Of course, having the cup kept so near the potential of the outside region helped in this regard, also.

That pick-up and rectification of A.C. was not a source of error in the current measurement was borne out by the agreement between calibrations made with and without the cyclotron R.F. on. To achieve this result, however, it was necessary to use filters at both ends of the cable connecting the Faraday cup to the electrometer.

Similarly, calibrations made using the cable and with and without the cyclotron beam on showed that ion collection in the cable was not a source of error. However, a more likely place for ion collection would have been at the connection between the Faraday cup and the electrometer cable. To minimize the air space around this junction, the

electrometer cable connector was soldered directly to the kovar vacuum seal which was connected with the cup, and the shield put around this connection was made as small as possible. The amount of ionizing radiation in this area was greatly reduced by having the beam stop in carbon, in which relatively few reactions could be produced. Since in addition the lead was kept near ground potential, the collection of ions there could not have been a source of error.

An opposite error could have arisen from the ejection of electrons from the outside rear of the cup by the gamma rays resulting from the stopping of the protons. This loss was, however, unimportant because (1) relatively few gammas were produced in the carbon and (2) most such electrons would have been returned to the cup by the magnetic field.

In considering whether a part of the proton beam could have missed the Faraday cup, it was important first to be sure the Faraday cup system was properly centered with respect to the beam. The accurately bored beam exit hole in the chamber wall provided the basis for this centering. The accuracy of this bore was checked both optically with a transit when the collimator was being aligned, and photographically with the beam itself. With the foil and guard ring removed, the cup was positioned by means of a cylinder turned so that one end fitted the chamber bore and the other end fitted the cup entrance. The cup housing was then screwed onto the chamber and alignment markings made, the use of dowelpins here being impracticable. The cup was held in the housing, or outer cylinder, by its electrical connection on one end (a 0.1" brass rod which was soldered into a kovar-glass seal in the housing) and by three teflon spacers at the other, or entrance, end.

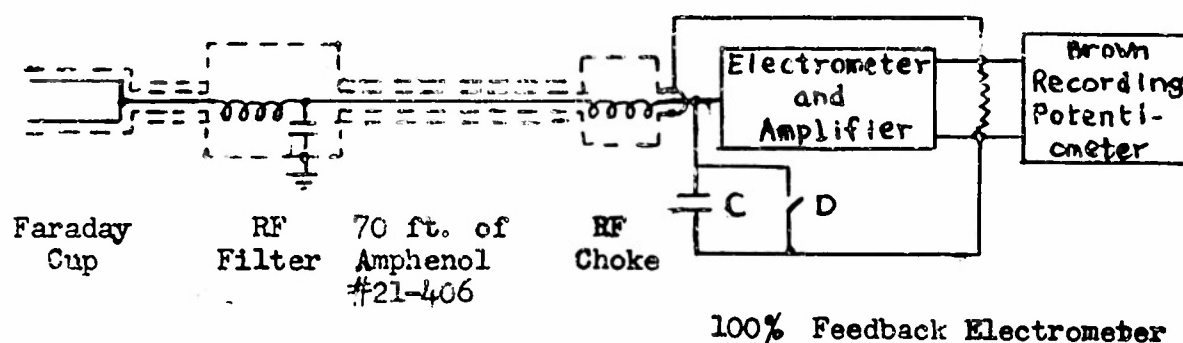
We can consider the question of loss calculations, having been assured of the centering of the collecting system. Losses have been calculated for both multiple and single scattering, the latter becoming more important than seems to be realized generally when considering losses smaller than one per cent. Although the effect of the deuterium was also included, most of the scattering took place in the Al exit foil. The aperture which determined the loss was the cup entrance, since the guard ring, although having a smaller opening, was made to subtend a larger angle at the foil. The result of the calculations is that, even assuming the beam to be uniformly dense out to the limit of the penumbra determined by the collimator, the losses were completely negligible. It turned out that on all sides of this beam at the cup entrance there was a space equivalent to about  $40 Y_{rms}$ , where  $Y_{rms}$  is the root mean square spatial displacement due to multiple scattering. Actually the situation was even better than this, since the beam entering the chamber was nearly parallel. Pictures showed that nearly all of the beam at the exit foil was contained within a circle of diameter 0.18", whereas the geometrical penumbra would have extended to 0.27".

The last of the nine errors in beam collection to be considered is that of having a part of the beam penetrate a portion of the collimating diaphragms and lose so much energy that the scattering events it produces are not counted. This unwanted part of the beam,



which undergoes more multiple scattering because of its lower energy, was partly eliminated by the last anti-scattering hole on the collimator and partly by having the chamber exit hole as small as possible, commensurate with not losing desired beam. The extent of slit penetration was decreased by using brass (cf. p. 13) slits of just a stopping thickness and by decreasing the number of protons striking the slits by using pre-collimating anti-scattering holes. A good measure of the amount of such low energy protons in the collected beam is given by the integral range curves obtained for the scattered beam (cf. p. 18). Within the 1% statistical error in the determination of each point on the curves, the integral range curve was flat for ranges smaller than the absorber thickness used at that angle. Despite there being no evidence for a low energy beam component, the total error assigned to the beam collection, 0.3%, is mainly to allow for such an effect. An even larger error, 0.5%, has been assigned for measurements made when the beam had shifted, an occurrence which will be discussed later.

Since the current-integrating electrometer had to be located in the cyclotron control room, about seventy feet of cable was needed to connect to the Faraday cup. Like the cables from the preamplifiers, the electrometer cable went through a conduit, but unlike the other cables it had a double shield and was made especially for this purpose by Amphenol (#21-406). Such a length of cable would present many problems with the low beam currents used were it not that the electrometer kept the voltage across the cable essentially at zero. The electrometer was the University of California (Berkeley) Radiation Laboratory's Model II, with a few modifications to improve stability. The action of the circuit has already been described, but perhaps a clearer idea of the function of the various parts of the feed-back, slide-back system can be obtained from the following simplified diagram.



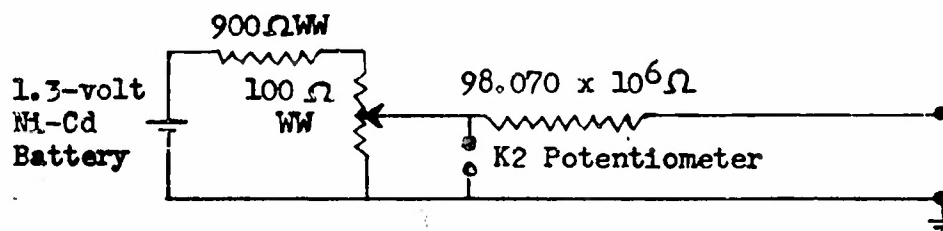
The filtering was found to be necessary to eliminate all effects of cyclotron RF pickup, as has been previously discussed. The choke at the cup end was 7 mh and at the electrometer end, 10 mh, while the filter condenser was .001  $\mu$ f. The capacitance of this condenser, as well as the 80  $\mu$ f of the cup and the .0008  $\mu$ f of the cable were made completely negligible compared to the integrating capacitor, C (usually

0.1  $\mu\text{f}$ , but .01 $\mu\text{f}$  for a few runs), by the feed back action of the electrometer. Since the gain of the electrometer was about 550, the effective capacitance of the cable, filter, and cup was only about .000003  $\mu\text{f}$ , exclusive of the small effect of electrometer zero drift.

The filter condenser and the integrating condensers were all Fast polystyrene capacitors, which were found to have quite small leakage and soakage. The electrometer tube was a Victoreen 5803, having a grid current of about  $2 \times 10^{-13}$  amp. The function of the condenser dumping switch, D, which shorted out the capacitor after its voltage had reached a pre-set value (as determined by the Brown Electronik Recording Potentiometer), has already been described in detail. The potentiometer was frequently made to check itself against a standard cell.

Having discussed the method of beam collection and integration, we shall next consider the calibration of the integration system. The problem of making an accurate calibration for currents of the order of  $10^{-10}$  to  $10^{-11}$  amp. is rather a difficult one. The easiest way out is to determine the integrating condenser capacitance, but this frequently used method is not very reliable, both because the effective capacity value frequently depends on the procedure used in the determination, and also because the capacity of even polystyrene condensers often can change by as much as 3/4% within a few months.<sup>111</sup> On the other hand, if one can use a current-time method, employing currents of the same size as the beam currents measured, then many sources of error -- such as additional capacitances, leakage, soakage, electrometer tube grid current, and condenser discharge time -- are taken care of. While the current-time method is not new, it is believed that it has never before been used to obtain accurate calibrations with such low currents.

The form of calibration circuit which was finally used is given here:



It was necessary to use the K2 potentiometer across a low impedance to achieve large enough galvanometer deflections when obtaining balance conditions. The large precision resistance was made up of 98 one-megohm "Evenohm" resistors, having a temperature coefficient of  $\pm .000025/^{\circ}\text{C}$ . Each resistor was measured to about .01% at  $25^{\circ}\text{C}$  by the manufacturer (Cinema Engineering Co., Burbank, Calif.), using a Leeds and Northrup Anthony-Pattern Bridge. The resistors were assembled in groups between steatite posts projecting from Lucite sheets, which in turn were positioned inside a double box. Glass



wool, for thermal insulation, was placed between the inner Lucite box and the outer aluminum box. The humidity inside the double box was kept low with silica-gel. Extensive tests were made to be sure that all possible electrical leakage paths gave a negligible effect. An over-all check on the value of the assembled resistors was made to an accuracy of about 0.1% by bridging the resistance box against two resistors calibrated by the National Bureau of Standards.

Neither the value of the  $10^8$  ohm resistance, nor the value of the voltage, as measured by the K2, limited the accuracy of the calibration method. Since the timer (see Fig. 5) was turned on and off by the same relay which controlled the condenser shorting switch, measuring the time required for a condenser charging cycle also did not limit the accuracy. Once all sources of pick-up had been eliminated, the limitation on the calibration accuracy was imposed by the zero drift of the electrometer and by the build-up of voltage across the integrating condenser during the charging cycle.

The electrometer zero could be set before each run, but any resulting zero drift could be measured only after the run. Such zero drift had two effects. One effect, the voltage as measured by the Brown Recording Potentiometer being not quite the same as the voltage across the condenser, was small and could be accurately corrected for, since it involved knowing only the final value of the zero drift. This first effect also had to be corrected for when making beam current integrations. The second and much more serious effect, however, was present only when using the calibrating circuit, for then the zero drift acted like a battery appearing at the grid of the electrometer tube. To correct for this added voltage, one had only the average value of the zero drift to use, whereas the drift of the electrometer zero usually occurred in an erratic, rather than a linear, fashion. The inaccuracy of this correction provided the main variation, from one run to another, in the value obtained for the charge per dump calibration constant ( $Q_d$ ). Because this effect of zero drift increased as the circuit voltage was made lower and the dumping time became longer, reliable calibrations for the 0.1  $\mu\text{f}$  condenser could not be obtained for currents smaller than  $10^{-11}$  amp. However, only the  $8^\circ$  proton runs were made with currents any smaller than that.

Because of the high gain of the electrometer, even at  $10^{-11}$  amp. the effect of voltage build-up on the condenser required only an 8% correction when calibrating the 0.1  $\mu\text{f}$  condenser. Since the electrometer gain could be measured (using a low-impedance voltage source, calibrated with a K2) to 1% just prior to calibrating, and the condenser's capacitance was known to about 1/2%, the correction,  $1 - (t_d/2RCA) + 2(t_d/2RCA)^2/3 - \dots$  (where  $R = 98.070 \times 10^6$  ohms,  $A$  = electrometer gain,  $t_d$  = dumping time, and  $c$  = condenser capacitance), could be made with sufficient accuracy for the 0.1  $\mu\text{f}$  condenser. However, for very long dumping times with the .01  $\mu\text{f}$  condenser, this second limitation was more important than zero drift. However, with the exception of a few  $8^\circ$  deuteron runs, the .01  $\mu\text{f}$  condenser was not used with currents which were smaller than those which gave reliable calibrations.

The shape of the  $Q_d$  (charge per dump) vs.  $t_d$  curves for both condensers were such that quite good extrapolations could be made to lower current (i.e., larger  $t_d$ ) values. For the .01  $\mu\text{f}$  condenser,  $Q_d$  was found to be constant for dumping times of 150 to 700 seconds, while for the 0.1  $\mu\text{f}$  condenser,  $Q_d$  decreased slightly with  $t_d$ , indicating some soakage. For both condensers  $Q_d$  became larger for very short dumping times because the response of the Brown Recording Potentiometer was not rapid enough.

The absolute value of  $Q_d$  for the 0.1  $\mu\text{f}$  condenser at a particular current was checked in three ways. A duplicate calibration circuit using a  $10^8$  ohm Victoreen resistor calibrated by the Bureau of Standards gave a  $Q_d$  value 0.5% lower, which is within the accuracy of the resistor calibration. On the other hand, a  $Q_d$  value 0.5% higher was obtained by letting the integrating condenser discharge through a ballistic galvanometer and then calibrating the galvanometer using the constant current (resistance box) source and measurements of the galvanometer's period and logarithmic decrement. This agreement is also well within the expected error of the measurement. The final check on  $Q_d$  was obtained using a value for the condenser capacitance, found by both bridge and RC-time methods and known to about 0.5%, and the voltage at which the condenser was dumped. The latter was determined by checking the Brown potentiometer's reading with a low-impedance voltage source, calibrated by a K2 potentiometer, applied by breaking the electrometer's feedback loop. Using these values gave agreement to within 0.2% with the equivalent  $Q_d$  value obtained from the charge-time calibration.

In general, it is believed that the  $Q_d$  values have standard errors varying from 0.2% (for currents high enough so that the zero drift or condenser voltage effects were small) to 1% (for currents so low that an extrapolation of the  $Q_d$  curve was necessary). The error assignment is based on the absolute value checks and on the reproducibility of over three hundred calibrations made during the course of the experiment.

#### I. Vacuum system

Since the vacuum system was fairly conventional, it will not be described in any detail. The single system could be used to pump on both the scattering chamber and the Faraday cup, or either one separately. A Distillation Products, Inc. VMF-20A diffusion pump (with Octoil-S) was used with a Welch Duo-Seal mechanical pump for backing and roughing. Separate mechanical pumps were used for both the deuterium and counter filling systems. The mechanical pumps were kept on a cart separate from the one carrying the scattering chamber, the only connection between being made by rubber vacuum hoses. In this way, both mechanical vibrations and electrical disturbances could be greatly reduced.

While a liquid nitrogen trap was available, it was usually used only when it was necessary to pump down rapidly, for the whole system (including the chamber) could reach  $3 \times 10^{-5}$  and the Faraday cup alone,

$9 \times 10^{-6}$  mm. Hg without liquid nitrogen. With the trap filled, the whole system could get down to  $9 \times 10^{-6}$  and the cup alone,  $2 \times 10^{-6}$ . Liquid nitrogen was rarely needed to get the Faraday cup down to a good enough vacuum, for within a few minutes of shutting off the chamber the cup pressure was always about  $1 \times 10^{-5}$  mm. Hg.

To help determine the extent of contamination scattering and of changes in the partial pressure of deuterium, the rate of rise of the chamber was checked several times. In general, for the first few hours after shutting off the chamber from the pumps, the pressure increased about 0.3 micron/minute (or  $3 \times 10^{-4}$  mm. Hg/min.). For longer periods, the rate of rise was slower. The main contributor to this leak rate was probably the chamber itself, since this brass casting was found to be quite porous. Making the chamber reasonably tight provided the chief vacuum problem.

#### J. Deuterium system

To measure the differential scattering cross section it is necessary to know the number of scattering atoms present, and hence the pressure and temperature of the scattering gas and the percentage of deuterium in that gas. To eliminate all impurities initially except normal hydrogen, the deuterium gas was forced to diffuse through the walls of a heated tube of palladium. By using 150 lb/in.<sup>2</sup> deuterium pressure and 150 amp. through the Pd tube, the five-liter chamber could be filled in about twenty minutes. Because oxygen can diffuse through hot copper, the deuterium coming out of the hot Pd was passed through only stainless steel tubing to a liquid nitrogen trap. Besides cooling the hot gas, the liquid nitrogen served as a vacuum pump. Since the deuterium filling section was not opened to the air, except for rare repairs, it was sufficient to evacuate it prior to putting in a new filling to the pressure achieved by a mechanical pump and the liquid nitrogen trap.

The deuterium for the final runs was obtained shortly before it was used from the Stuart Oxygen Co., San Francisco. The two tanks used for nearly all of the data were later analyzed mass-spectrographically by the Consolidated Engineering Corp., Pasadena. The more impure of the two was found to contain only .04% air and .02% water, so the Pd tube was almost superfluous. The H<sub>2</sub>D analysis, which had a limit of error of less than .05 mol %, showed one tank contained 99.20 mol % D and the other 99.25%. The presence of H made necessary a small correction ( $0.45 \pm .06\%$  in the worst case) for those protons scattered from H which had an energy at the lowest angles such that they were counted along with protons scattered from D. This correction will be discussed in a later section.

Knowing the percentage of deuterium present, we next need to know the pressure of the entire gas. The chamber was filled until a Bourdon gauge indicated that the pressure was approximately equal to that of the atmosphere, whereupon the chamber was opened to the evacuated arms of a small glass U-tube manometer, half-filled with Octoil-S diffusion pump oil. After closing a stop-cock between the arms, the arm not

connected to the chamber was opened to the atmosphere. The resulting difference in the heights of the two oil columns gave the pressure differential between the chamber and the atmosphere. While this height difference was usually read with a cathetometer, such accuracy was not really needed, since a millimeter error in measurement would have given only .01% error in the pressure.

Octoil-S was chosen as the manometer oil because (1) it has an extremely low vapor pressure ( $5 \times 10^{-8}$  mm. at 25°C.), (2) it is a saturated hydrocarbon and hence dissolves much less gas than if it contained any double bonds, and (3) its density and variation of density with temperature are well known. Using the average of density determinations made by the manufacturer (Distillation Products, Inc.) and by two other groups,<sup>8, 11, 12</sup> all of which agree within .01%, plus the local value of gravity (known to  $\pm .002\%$ ), we get that the pressure differential in millibars is  $0.8918 [1 - .00073 (T - 25^\circ\text{C.})] M$ , where M is the difference in the manometer arm heights in cm. and T is the temperature in °C.

The atmospheric pressure near the chamber was measured with a Friez Aneroid Barometer\* to 0.1 mb. While the aneroid was checked quite frequently against the U.C.L.A. Meteorology Department's standard mercury barometer (which in turn had been checked against local Weather Bureau and Air Force standards), it was found that the readings of the two, when properly corrected, agreed to within about  $\pm 0.2$  mb. over a period of nearly nine months. The over-all error in the absolute measurement of the gas pressure in the chamber is estimated at  $\pm 0.4$  mb., or  $\pm .04\%$ .

It is believed that the measurement of the gas temperature was even more accurate, being about  $\pm .03\%$ . An 18-35°C. thermometer, made by the Parr Instrument Co. (Moline, Ill.) and graduated in .02° intervals, was used. While a calibration curve supplied by the manufacturer makes possible obtaining differential temperature errors of only .002°, the absolute values are good to .02°, and so readings were made to just .01°. An error of .02° is an error of only .007% in the absolute temperature, but the larger error given above results from the uncertainty as to whether temperature equilibrium between the gas and its surroundings had been established before simultaneously reading the temperature and pressure. Errors resulting from a lack of temperature equilibrium could not have been very large, however. The chamber filling time was fairly slow, and the gas had to pass through a long copper coil after leaving the liquid nitrogen trap and before entering the chamber. Furthermore, the Parr thermometer passed through an O-ring seal in the lid of the chamber, so that its bulb was immersed in the gas close to the scattering volume. A temperature reading was made only when the Parr thermometer and one outside the chamber agreed to within 0.1°.

---

\* We wish to thank Dr. James Edinger of the U.C.L.A. Meteorology Department for the loan of the aneroid and the use of both the standard mercury barometer and the Gaertner traveling microscope, previously mentioned.

Readings of the temperature and pressure were made both at the beginning and end of the period during which the gas was used, and the resulting difference in T/P values was compared with the expected leak rate of the chamber, taken from rate-of-rise measurements. Usually, T/P changed by about .006% per hour, and T/P values were assigned to each run according to the time elapsed since the chamber was filled. Usually fillings were used for one and sometimes two nights, so that this correction for the change in T/P was always quite small.

In general, the error in T/P for most runs was taken to be 0.1%, although in a few cases a somewhat larger error was assigned.

#### IV. PROCEDURE AND EXPERIMENTAL CHECKS

We have discussed the various parts of the equipment separately, now we shall consider the operation and checking of the apparatus as a whole. We have, for example, examined the aligning of the collimator, Faraday cup, etc., but we should also mention the alignment of the entire scattering chamber.

A diaphragm with a small hole in it was placed over the end of the external beam exit pipe so that the hole was at the position of the most intense beam, as determined by beam pictures and beam current measurements. Another evacuated section, about five feet long and having a glass end, was added to the exit pipe, beyond the diaphragm. By bombarding the glass for a few minutes with the proton beam, a darkened image of the hole in the diaphragm appeared on the glass. After aligning a transit along the line formed by the centers of the diaphragm hole and its image on the glass, the scattering chamber was moved in so that the axis of the collimator was also along this line. This was determined by sighting the transit on the collimator defining holes through the chamber exit hole, with the Faraday cup removed. Minor adjustments were then made in the chamber's position, in accordance with beam pictures taken inside the evacuated chamber.

With the chamber in place and the cyclotron's magnetic field on, a flux-meter survey was made to determine whether the magnetic field inside the scattering chamber could cause any scattered protons to fail to properly pass through the counter analyzing slits. While the cyclotron's field, as previously mentioned, turned out to be negligible, the stray field from the magnet at the Faraday cup entrance could have produced a small effect at the lowest angles. As can be seen from Fig. 3, three shims were placed around this magnet to achieve the double purpose of reducing the field inside the chamber and of providing a strong field in the region of the chamber exit foil.

Having considered the procedure for getting the chamber ready to use, we shall now briefly discuss the procedure followed in a typical night of data taking. First, the vacuums of the chamber and deuterium filling systems were checked to be sure that no leaks had developed. While the chamber was being filled through the heated Pd tube, the electronic system was checked. Pulses from a mercury-relay pulse generator were applied simultaneously to all three counting channels. By switching the accidental coincidence circuit so that it counted real double coincidences, the performance of all five scalers could be checked at once. The operation and linearity of the upper and lower level pulse-height discriminators were checked by using two sizes of pulses from the accurately calibrated pulse generator. It was important to be sure that each discriminator "slope" was set so that the desired range of pulse heights could be included.



The pressure and temperature of the filled chamber were measured in a manner that has already been described (p. 32). A fresh filling was put in the counters and the high voltage measured and applied. Neither the counter high voltage supply nor any of the rest of the electronic equipment was ever turned off, except to make repairs. After setting the counter angle, the Faraday cup vacuum was measured, and then the cyclotron beam was maximized.

With beam into the chamber, the singles counting rate of the first counter was displayed on an oscilloscope. Most of the pulses were confined to a recurring group of about 20  $\mu$ sec. duration, which demarcated the cyclotron beam pulse. By making the output of the Master Pulser blank the oscilloscope trace, the 60  $\mu$ sec. scaler gating pulse could be set in proper time relation; i.e., so that the cyclotron beam pulse was at its center. It was then certain that the scalers were missing none of the desired counts while excluding some noise counts.

Before starting to collect data, the amplifier gains and discriminator levels had to be set. The usual procedure is just to try to set a lower discriminator level sufficiently low so that none of the desired counts are missed. In the present experiment such a procedure was undesirable because better particle selection was necessary, particularly when counting recoil deuterons. In addition, the usual method would have been far too time consuming, since counting rate plateaus would have to have been established for all three counting channels and for both upper and lower level discriminator settings in the first two channels. Instead, a quicker, more accurate method was developed, based on the calculated energy loss distribution<sup>100</sup> in the first two counters (as discussed on p. 8 and plotted in Fig. 4) and, for the third counter, also on the straggling calculations<sup>103</sup> mentioned on p. 18. The latter provided a means of determining the maximum energy which a particle could have after passing through a given thickness of absorber. Then, with the aid of the energy loss distribution curve, the minimum possible energy loss which a desired particle could have in the third counter was determined. Plots of this minimum energy loss vs. counter angle for protons and deuterons provided an accurate and easy way to get the initial approximate setting of the third counter discriminator, based on a previous run.

Approximate settings from any prior run could also be obtained for the first two counting channels, using a curve like Fig. 4. These settings were made quite generously and were not crucial, it not being a requirement of the method that the energy loss equivalent of a discriminator setting be constant over a long period. A run was then made to get the approximate counting rate at that angle. Next, the lower level first channel discriminator was set at some arbitrary higher level and another run made. From the difference in the counting rates of the two runs, the percentage loss caused by raising the first channel bias level was determined. Suppose we were counting 16-Mev protons and raising the first channel discriminator to a setting of 200 had decreased the counting rate by 30%. Fig. 4 shows that this discriminator setting of 200 must have corresponded to a 20 kev energy loss in the counter. Since the energy loss distribution essentially begins (0.1% curve) at 14 kev and ends

(99.9% curve) at 52 kev, the lower level discriminator had to be set below  $200(14/20) = 140$  and the upper level had to be set above  $200(52/20) = 520$ .

The second channel was set in the same way, but the third channel, because of the large range of energies in the third counter which resulted from straggling, had to be set by taking a conventional bias curve and finding a counting rate plateau. However, because the approximate setting was already known, usually just a few properly chosen settings sufficed to establish the plateau. Because the initial settings were usually fairly close to the final values, it was not often necessary to repeat the first and second channel setting determinations after finding the correct setting for the third channel. However, to guard against amplifier gain changes, these settings were usually checked during the course of data taking.

This method of discriminator setting had an additional use when counting recoil deuterons. Because of the broadness of the energy loss distribution, not all the protons from deuteron breakup having a range equal to or longer than that for the deuterons could be excluded. Hence it was necessary to make a background subtraction by using absorbers just thick enough to stop the deuterons. Since the group of inelastic protons being counted had a slightly higher energy than the group which actually constituted the background, it was necessary to reset the discriminators a little. These new settings were obtained easily using the energy loss distribution and third counter minimum energy loss curves.

The accuracy of this method of setting discriminators depends upon the linearity of the amplifier-discriminator system and on the correctness of Symon's energy loss calculations.<sup>100</sup> The first requirement was, of course, satisfied by the previously described nightly pulse generator check. The second was verified by the work of Igo, Clark and Eisberg,<sup>113</sup> who used a proportional counter similar to those employed in the present experiment, and who found quite close agreement with a curve calculated from Symon's theory at their energy of 31.5 Mev. Both requirements were actually checked nightly, once the discriminators were set, by predicting a discriminator setting for a certain percentage particle loss and then making a run to see if that loss was obtained. The empirical loss always agreed with the theoretical one within the statistical errors in the number of counts, which ranged from 3 to 6%.

With the discriminators set, data taking could begin. Short runs were made, usually lasting ten minutes or less, depending upon the beam current and the electrometer zero drift. Triple coincidences, accidental coincidences, the singles counting rate in all three counters, the number of condenser charging cycles (or dumps), the time, the run duration, and the electrometer zero drift were recorded for each run. The five scalars, timer, and condenser dump register all were simultaneously turned on by the Master Switch at the start of one condenser charging cycle and off at the end of the same or another cycle. During



periods when the cyclotron magnet had to be cooled, the electrometer was calibrated. At the end of using the chamber filling, the temperature and pressure of the gas were again determined.

Of the many experimental checks which were made and which will now be briefly described, perhaps the most important was that on the reproducibility of the data afforded both by having taken a number of short runs at each angle, and also, for the majority of angles, by having taken data at the same angle on different nights, sometimes weeks apart. For each angle, then, two statistical errors in the data could be computed: a poissonian one based on the total number of counts, and a gaussian one based on the reproducibility of the data. These two errors were compared by a chi-square test, and with a very few exceptions it was found that the data reproducibility depended only upon the number of counts. That is to say, for nearly all the runs the internal consistency of the data showed no errors outside the poissonian uncertainty in the total number of counts. The few exceptions were mainly runs for which it was found that a faulty relay had been erratically throwing extra counts into the scalers. While a good average background was found which corrected for this, the individual runs showed too much variation. An appropriately larger error has been assigned to these runs.

Another useful check on the reproducibility of the data was provided by counting both scattered protons and recoil deuterons at nearly the same center of mass angle. Among other things, this served as a good check on the deuteron background measurement, mentioned above. Because the two deuteron check points lie near the main minimum in the differential cross section curve, the inelastic background is relatively much larger compared to the elastic scattering at these two points than it is at lower laboratory (or higher center of mass) angles. Indeed, the main group of deuteron points ( $\theta \gg 130^\circ$ ) joins smoothly on to the proton points ( $\theta \ll 120^\circ$ ) right in the minimum, and the point at  $\theta = 130^\circ$  had a much larger background than did any other deuteron measurement. The deuteron check point at  $\theta = 89.9^\circ$  which is close to a proton point at  $\theta = 91.9^\circ$ , lies on a smooth curve drawn through the proton data.

This agreement of the deuteron data at  $90^\circ$  and  $130^\circ$  with the proton data has an added significance, since in one case the proton had a considerably higher energy than the corresponding deuteron, and in the other case the deuteron had over twice as much energy as the corresponding proton. Since the root mean square multiple scattering angle varies approximately inversely as the particle energy, if there were any appreciable multiple scattering loss (cf. p. 18) at any angle, it should show up in these two cases. This conclusion is made even stronger by the fact that the deuteron energy in one case and the proton energy in the other case were the lowest deuteron and proton energies used in the experiment, and therefore should have given multiple scattering losses if any were to be found.

Since at a fixed energy the multiple scattering loss would have been greater with the narrow slits than with the wide, both the proton and deuteron measurements at a laboratory angle of  $20^\circ$  were made with

narrow and wide slits as a further check. For the deuteron case the statistical errors were rather high, being 1.6% for the wide slits and 4.7% for the narrow, but the disagreement, 1.2% is in the opposite direction to that expected from multiple scattering. For the proton check the statistical errors were only 0.63% for the wide slits and 1.4% for the narrow, and the narrow slit cross section was 0.87% lower than the wide. The agreement of the wide and narrow slit data, then, shows again that multiple scattering losses were unimportant.

Still another check on multiple scattering loss was provided by making a 20° (laboratory) narrow slit proton run with the chamber filled with half an atmosphere of deuterium, instead of the usual atmosphere. Because this angle was the highest (and the proton energy the lowest) at which narrow slits were used, it afforded some test of multiple scattering losses in the gas. However, because calculations show that the loss in the gas ought to be quite small, and because the angle is fairly low, this served as a better check that scattering from the collimating slits to the analyzing slits was not affecting the results. Since the slit-slit scattering and the multiple scattering effect would both cause the cross section found with a half-atmosphere filling to be higher, an upper limit on both effects is determined by the fact that the half-atmosphere data (1.0% statistical error) was 0.22% lower than that obtained with a full atmosphere filling (1.4% statistical error).

Another good check on slit-slit scattering effects was accidentally provided by a shift in the direction at which the beam entered the collimator. This direction shift caused a large increase in the number of protons striking the edges of the last defining hole in the collimator. Some of these protons, scattering off various metal surfaces, found their way into the first and second counters. However, these protons must have lost too much energy in the many scatterings to have been able to get through the absorber in front of the third counter, for measurements made after the chamber was realigned to the new beam direction agreed within statistical error with those made before realignment. For example, the deuteron measurements at 12.5° (laboratory) show that despite the fact the first and second counter counting rates decreased by a factor of over two after realigning, the cross sections obtained before and after realignment agreed within 1.4%, for statistical errors of 1.3% and 1.1%, respectively. Similarly, while the singles rates went down by a factor of two after realigning, the cross section for protons measured at a laboratory angle of 10° went up 0.82%, for statistical errors in the two measurements of 1.9% and 1.4%.

Thus slit-slit scattering was not a source of error in the cross section measurements, with one exception. At 8° neither the last anti-scattering hole in the collimator nor the anti-scattering baffle was effective in keeping protons scattered off the second collimator defining hole from getting through the first analyzing slit. The only importance of this when counting protons at this angle was that it increased the singles rates in the first two counters, and consequently necessitated running at smaller cyclotron beam currents. However,

when counting deuterons the absorber used was thin enough to admit some of these slit-scattered protons. Thus the ratio of background to total counts was about six times as large at  $8^\circ$  as it was at  $10^\circ$ . Not only did this high background make the  $8^\circ$  runs statistically more inaccurate, but also it was found that the slit-scattered proton background decreased rapidly with energy. A correction for this had to be made by filling the chamber with ordinary hydrogen and making runs with the same absorbers and discriminator settings as were used when taking deuteron and background counts. A rather large error in the backgrounds was assigned for this correction.

While background measurements were made for all deuteron runs, only a few were taken for proton runs, since proton backgrounds were nearly always found to be negligible. These few were done in the same manner as for the deuteron runs: i.e., just enough extra absorber was used to stop all the p-d elastically scattered protons. This lack of background showed the absence of a number of undesirable effects: (1) slit-slit robbing, (2) scattering from heavy contaminants, (3) false triple coincidences as a result of neutron recoil background, and (4) noise counts due to electrical disturbances. The only backgrounds found exceeding accidental coincidences were due to electrical disturbances (e.g., bad Des sparking), since the net background was zero when the source of the disturbance was fixed.

These proton background measurements served also as a check on the method of determining accidental coincidences, since with a stopping, or background, absorber in place the triple coincidence and accidental coincidence counts were essentially the same.

However, the average accidental coincidence correction for any angle was never as large as 2%, mainly because at the smallest angles the beam current had to be reduced (by reducing the hydrogen supply for the  $\alpha$  deuteron arc) to prevent counting losses. Runs were made of cross section versus beam current to determine the maximum singles counting rate which could be tolerated before losses occurred. When getting data at small angles, the scalars recording the singles rates were constantly watched to be sure that the rate was staying well below the safe limit.

Runs at any angle which were made with quite different beam currents served as a good test of the current integrator calibration, since each run was assigned its calibration constant on the basis of the run duration (i.e., the charging time of the integrating condenser). A further check was provided by making runs with two different (0.1  $\mu$ f and .01  $\mu$ f) integrating condensers. Regardless of having different beam currents or different condensers, the cross section values always agreed well within statistical errors.

The cross section at a given angle was measured as a function not only of beam current, but also of coincidence resolving time (as described on p. 21) and elapsed time. A decrease in the cross section with time could have been ascribed to amplifier gain changes or counter gas contamination. The former had to be carefully watched during each

night's data taking, while the latter was checked by making runs with gas which had been left in the counters three times as long as it normally was.

An increase in cross section with time could have been attributed to an increase of scattering from air, due to the leak rate of the chamber. As mentioned above, any such increase could be checked by making background measurements on the proton runs. Still another check was made by using an appropriate absorber, to measure the scattering from air at  $25^\circ$  periodically during a night of data-taking. By measuring also the cross section for scattering at that angle with only air in the chamber, the increase in the air concentration could be determined directly and checked with the leak rate of the chamber. The effects of contamination scattering were found always to be very small, and it turned out that a sufficiently accurate correction to the data at the lowest angles for such scattering could be made simply by using the measured chamber leak rate, as checked or slightly modified by the change in the temperature/pressure readings made at the beginning and end of the period during which a gas filling was used (cf. p. 34).

One conventional check is to measure a cross section at the same angle on both sides of the beam. This test of the alignment is best made at a small angle, but with the present equipment the smallest angle at which counting could be done on both sides of the beam was  $45^\circ$ . The agreement in the two cross section determinations at that angle was within 0.15%, which is much better than the statistical accuracy of the measurements.

A desirable over-all check is to measure a cross section which someone else has already measured accurately. No such check is yet available at this energy, but Herbert N. Royden of this laboratory is measuring p-p scattering at low angles. Since his results are not yet available, the p-p check run, which was made at a laboratory angle of  $20^\circ$ , can be compared with a  $1/E$  interpolation between the 18.3-Mev<sup>111</sup> and 32-Mev<sup>114</sup> p-p measurements, as fitted by Martin and<sup>93</sup> Verlet with a Lévy potential. The agreement between the measured value, 24.0 mb./sterad. in the center of mass system, and the value obtained by interpolation, 23.9, is much better than the uncertainty in the interpolated value.

## V. RESULTS

### A. Corrections to the data

In the course of the foregoing discussion of the equipment and its use, mention has been made of various corrections which had to be applied to the data. Here we summarize these, giving references to the pages on which any correction is more fully discussed.

Background (pp. 37, 38, 40) was measured by putting just enough absorber in front of the third counter to exclude the particles having the previously desired energy. Because of the inelastic proton continuum, backgrounds had to be subtracted for all deuteron runs. For protons, on the other hand, measured backgrounds were generally negligible. In a few cases (p. 38), however, electrical disturbances necessitated a background subtraction.

All the data have been corrected for accidental coincidences (pp. 23, 40) by means of a coincidence circuit just like that used for registering triple coincidences, but connected so as to register whenever pulses from each of the first two counters occurred simultaneously with a delayed pulse from the third counter. This method was necessary because a large part ( $1/5$  to  $1/2$ , depending on the angle) of the pulses from the first two counters were in double coincidence. This large proportion of non-random counts was due, first, to the first two counters having a much larger solid angle than that of the second analyzing slit (which selected real triple coincidences), and secondly, at small angles, to protons which scattered from many metal surfaces and got into the first two counters. The correctness of this method for obtaining accidentals was checked experimentally (p. 40) and theoretically, using a formula (given in the Appendix) for the accidental counts in a system of  $n$  counters operating with a square-pulsed source. This formula, derived following the method used by Feather<sup>25</sup> for two counters, was used with  $n = 2$  and  $3$  and the measured values of single and double coincidence counting rates. The  $n = 3$  contribution was much smaller than that for  $n = 2$ , which was based on the 1-2 doubles and the 3 singles rates, and which gave good agreement with the electronic determination. The electronic method did require a correction of about 10% for the probability that counts were missed because the delay line kept the accidental coincidence system dead for the first part of the beam pulse. The formula for this is also given in the Appendix.

All the data also were corrected for electrometer zero drift (p. 30), the final value of the drift being read on the Brown Recording Potentiometer immediately after each run. Because the runs were kept quite short, the drift correction only very rarely was as large as 1%.

The temperature/pressure ratio (p. 34) had to be adjusted for each run on the basis of the rate of rise of the chamber and the measurements of T/P which were made at the beginning and end of using a gas filling. The correction to the T/P reading was very small, changing by about .006% per hour.

The same rate of change of T/P was used to determine the rate of increase in scattering from air contamination. Experimental checks (p. 41) confirmed that this effect was small, and corrections were made only for proton runs at angles of  $17.5^\circ$  or less. The only corrections exceeding 0.1% were those at  $8^\circ$  (0.34%) and  $10^\circ$  (0.18%). The smallness of this effect was due, at small angles, to using deuterium fillings for only a short time, and at larger angles, to discriminating against the higher energy air-scattered protons.

Another source of additional counts for which a correction was necessary was the presence of ordinary hydrogen in the gas. The amount of hydrogen was small (about 0.8%) and accurately known from mass spectroscopic analysis (p. 32). To obtain a good correction, it was necessary to know also the p-p scattering cross section and the percentage of p-p protons at each angle excluded by the absorbers. The cross sections were obtained from an interpolation between the curves given by Martin and Verlet<sup>93</sup> (cf. p. 41). The energy resolution of the absorbers was determined by folding the nearly gaussian distribution in range due to straggling<sup>103</sup> with the trapezoidal distribution due to the angular resolution of the analyzing slit system. The accuracy of the latter calculation was confirmed by the shape of integral range curves obtained experimentally. In general, then, the correction for hydrogen contamination was small and accurately known. Because of the energy resolution of the absorbers, only proton angles of  $20^\circ$  or less had to be corrected, and the largest correction was  $0.45 \pm .06\%$ .

A larger correction was that for the loss of particles in the absorbers. While the loss due to multiple scattering was negligible (p. 18), losses due to single scattering and absorption had to be considered. Cross sections for proton and deuteron absorption in Al as a function of energy were computed from the work of Shapiro,<sup>116</sup> and were numerically integrated with respect to range. The resulting curves are proportional to the fractional beam loss due to absorption, as a function of absorber thickness. A similar procedure was followed for single scattering, with added complications. Experimental differential cross sections for p-Al at 22,<sup>117</sup> 18,<sup>118</sup> and 9.6<sup>119</sup> Mev and d-Al at 14 Mev<sup>120</sup> were used along with calculated Rutherford cross sections to determine the energy dependence of the scattering cross sections. All of the differential cross sections had to be multiplied by a cut-off factor which was a measure of the probability a particle scattering at a certain angle in the Al absorber had of missing the third counter. This probability factor was determined by a quadruple numerical integration over the areas of the beam in the absorber and of the third counter opening. The cut off differential cross sections were integrated with respect to solid angle and then plotted as a function of range, from which point the scattering and absorption corrections



proceeded in the same way. Only at the lowest energies (and consequently thinnest absorbers) did the scattering loss approach that for absorption. Where the correction is large, only the absorption is important. Corrections varied from 1.02% for protons at 8° to 0.08% for protons at 90°.

An opposite correction had to be applied for the extra particles obtained because the analyzing slits could not be perfectly absorbing. For the second slit, the equations of Courant<sup>121</sup> could be used directly, but a correction for the first slit required in addition numerical integrations over the beam incident on the slit edges and over the two-dimensional gaussian distribution of particles which penetrated the slit edges. The first integration determined the number of protons striking the slit edges relative to the number going through the slit openings, and the second determined the fraction of particles penetrating the first slit with small energy loss which could get through the second slit. The resulting correction changed little with angle, varying from 0.41% for 8° protons to 0.17% for 45° deuterons, because of the method of choosing absorbers. The correction was small because, in approximate order of importance, (1) the discrimination of the counting system against lower energies was so good (p. 8), (2) the slits were made as wide as possible by making the distance between them as large as possible (p. 7), (3) the slits were made of high Cu bronze (p. 13), (4) the slit edges were just a stopping thickness for 20-Mev protons (p. 13), and (5) the number of particles striking the slit edges which could scatter from the gas at a smaller angle than the particles being counted were reduced both by the anti-scattering baffle (p. 16), and by having the collimator project as far as possible into the chamber (p. 12).

A large correction which also had to be applied to all the data was for the finite width and height of the incident and scattered beams. A second-order geometry analysis was kindly supplied by Prof. C. L. Critchfield, and some fourth-order terms in the rear slit height were added to it for this particular geometry (cf. Appendix). The resulting corrections ranged in magnitude from 3.83% for 8° protons to 0.03% for 85° protons.

### 7. Summary of errors

Like the corrections to the data, errors have been discussed in the preceding pages. The latter will be summarized here in relation to determining the cross section. Unless otherwise specified, all errors throughout this report are expressed either as standard deviations or relative standard deviations.

Looking at the differential laboratory cross section,  $\sigma_d(\theta_{lab}) = TC \sin \theta_{lab} / K G P F I Q_d$ , we can first dispose of K, the universal physical constants. The constants used, obtained from DuMond and Cohen,<sup>122</sup> and consisting of the gas constant, Avogadro's number, and the electronic charge, are known so accurately that they introduce no error here.



To determine the number of scattering targets, we need to know the temperature,  $T$ , and pressure,  $P$ , of the gas, and the fraction,  $F$ , of the gas which is deuterium.  $F$  was found mass spectroscopically (p. 32) with a limit of error of .05 mol%. Errors were designated for the ratio  $T/P$ , since the error had to include uncertainties in the measurement of  $T$  and  $P$  and in the change of  $T/P$  with time (p. 34), an individual  $T/P$  being assigned to each run. Since the changes in  $T/P$  were small (p. 34) and the measurements (p. 33) were quite accurate, an error in  $T/P$  of 0.1% was assigned for most of the runs, with a somewhat larger error for a few.

A small (.07%) Van der Waal's correction was made in the cross section formula for deuterium's deviation from perfect gas behavior, but of course, no error need be assigned to this.

The number of incident particles was determined by the beam current collected, which was measured by the number of condenser dumps,  $I$ , and the charge per dump,  $Q_d$ . Individual  $Q_d$  values and errors were assigned to each run on the basis of the beam current, as measured by the time required for a dump. These errors (p. 31) varied from 0.2% for high currents to 1% for very low ones. In addition, nearly all runs have been assigned an error of 0.3% (and the rest, 0.5%) for possible errors in beam collection (p. 28).

The portion of the scattered beam seen by the counting system is determined approximately by  $\sin \theta_0 / G$ , where  $\theta_0$  is the angle the counter makes with the incident beam and  $G$  includes the constant geometrical factors. The combined errors in the measurement of the constants of which  $G$  is comprised and in the alignment of the counter slit system amount to only .047% for the wide slits and 0.19% for the narrow (p. 15). However, the uncertainties in  $\theta_0$ , while only .063° for the narrow slits and .066° for the wide, give an error in the cross section which varies from 0.13% at 90° to 0.79% at 8° (p. 16). A similar large error, which also varies with angle, arises from the uncertainty in the centering of the incident beam. This latter error (p. 13), with a few exceptions, is given by .064%/sin $\theta_0$ . The exceptions, for which the error has been doubled, are those runs made when the cyclotron beam direction had shifted (p. 39). This shift skewed the incident beam, and the added error is considered to represent the shift in the beam's effective center at the chamber center.

The largest error in the cross section arose from the determination of the number,  $C$ , of properly scattered particles counted. There were several small contributors to this error, among which was the background correction (p. 42) made for all deuteron and a few proton runs. Besides the additional statistical uncertainty which the background introduced and which will be discussed later, an error of about 5% of the deuteron background correction has been included as an allowance for the fact that the part of the inelastic proton distribution measured as a background was of a slightly higher energy than the part which actually constituted the background. It has been

found experimentally (p. 38) that this effect is small. The background subtraction for the few proton runs (p. 38) requiring it was much more uncertain, however, and an error of about one-third of the correction has been assigned. Similarly, a large error has been included for the unusual deuteron background at  $8^\circ$  (p. 40).

As was the case with background, the presence of accidental counts added to the statistical uncertainty in C. In addition, however, errors in the number of accidentals have been assigned as 10% for angles less than or equal to  $25^\circ$  and 20% for angles greater than  $25^\circ$  to take care of (1) the cyclotron beam pulses' not being strictly a square-wave time function, (2) the increased probability of getting an accidental because of the presence of real triples, and (3) the decrease in accidentals due to not recording entirely random accidental triples. These error assignments do not have much effect on the total cross section errors, since the correction for accidentals was usually much less than 1%, and only at one angle did it approach 2%.

The error in C due to a correction for electrometer zero drift was considered negligible, since the corrections were always quite small and could be made rather accurately. No error has been assigned for counting losses, either, since the beam current was always kept low enough to make these negligible (p. 40). In view of the theoretical calculations (p. 19) and the many experimental checks (pp. 38-39), multiple scattering losses can also be considered insignificant.

The main source of error in C and in the whole cross section determination was the poissonian nature of the number of counts. This relative statistical error in the most complicated case is given by

$$\frac{[(C_g + A_g)/I_g^2 + (C_b + A_b)/I_b^2]^{\frac{1}{2}}}{(C_g - A_g)/I_g - (C_b - A_b)/I_b},$$

where the subscript g refers to the measurement of the gross counts and b to the measurement of background alone, and C designates total counts (of which A were accidentals) in I condenser dumps. It must be reiterated (p. 38) that a gaussian statistical error, which measured the reproducibility of the data at each angle, was also computed and compared with the poissonian one, with the result that almost all the data showed no significant variation outside that expected on the basis of the number of counts involved.

After computing a cross section by the formula given, five additional corrections were applied, the errors of which must be considered. The error in the correction for scattering from air contamination (p. 43) was taken to be one-third of the correction, but in the worst case ( $8^\circ$  protons) this error amounts to only 0.11%. The largest error due to the correction for scattering from ordinary hydrogen (p. 43) was even less, .06%. The error in the third of these corrections, that for particle loss in the absorbers (p. 43), depends mainly upon

the accuracy of the theoretical absorption cross sections. While the energy dependence of these cross sections has been well checked experimentally,<sup>116</sup> there is more doubt about their absolute values. Consequently, an error of 30% of the correction has been assumed. This gives an error of 0.3% in the cross section in the worst case.

An error is not usually assigned to the correction for finite beam size (p. 44), but since derivatives of the imperfectly known cross section are involved in terms which tend to cancel, errors can result which are actually larger than the correction. An error of 6 of the correction has also been assigned to include the effects of neglected higher order terms and of the approximate treatment of the incident beam. The resulting errors in the cross section vary from 0.36% for 8° protons to .003% for 17.5° protons

Two errors must be considered in the fifth correction, that for slit-edge penetration. The error assigned to the correction made for the analyzing slits (p. 44) is taken to be half of the correction, because of the lack of better experimental verification of the theoretical treatment. The largest error this introduces in the cross section is 0.20% for 8° protons. The second error to be considered is that for neglecting collimator slit-edge penetration. First, it should be recalled that an error has already been assigned for the possibility that a small portion of the incident beam collected in the Faraday cup could have been of such a low energy, due to collimator slit-edge penetration, that it would not have given countable scattering events (cf. p. 27). However, it is also necessary to determine that fraction of the incident beam which could produce recordable scattering events of degraded energy. By a calculation similar to that for the analyzing slits, it was found that only 0.11% of the scatterings counted could have been of low energy, giving a maximum error in the cross section of .006%.

The various errors considered above have been combined quadratically, and the resulting relative standard deviation in the cross section for each angle, along with the cross section values, may be found in Table IV. It must be emphasized that these errors apply to the absolute values of the cross sections, since each determination was an absolute measurement. The error in relative values of the cross sections is not well defined, because the size of such an error would depend upon which two differential cross section values are being compared.

### C. Beam energy determination

Without an accurate determination of the energy of the beam at the center of the chamber, the cross sections would be of little value. In order to check the use and calibration of the absorbers as well as to determine the beam energy, the energy measurement was made by taking an integral range curve with the absorbers in front of the third counter, while counting protons from p-p scattering at 20° or 25°. Three such determinations were made during the course of the experiment.

There are three uncertainties in the energy: (1) the error in the mean energy determination, (2) the energy spread in the beam at any particular time, and (3) changes in the mean energy with time. Considering the first of these, there are three errors in the determination of the mean energy, uncertainties in (a) the absorber thickness, (b) the mean range determination, and (c) the range-energy relation. The main part of the  $1.5 \text{ mg./cm.}^2$  uncertainty in the absorber thickness came from assigning the equivalent stopping power of the counter gas and hydrogen, since the counter windows and the absorbers themselves were all weighed and measured accurately. The value of the mean range, as found both from the midpoint of the integral range curve and from the peak of a derived differential curve, also had an uncertainty of  $1.5 \text{ mg./cm.}^2$ . Adding these two contributions quadratically to the uncertainty in the range-energy relation of  $2.3 \text{ mg./cm.}^2$  gives an error in each mean energy determination of .08 Mev.

The range-energy relation used was computed for a mean ionization potential,  $I_{Al}$ , of  $164 \pm 3 \text{ ev}$ , as given by Caldwell and Richardson,<sup>123</sup> based on the energy-loss measurements of Sachs and Richardson<sup>124</sup> at 18 Mev. The range values were obtained by using the values of Smith<sup>125</sup> for  $I_{Al} = 150$ , corrected with the relation given by Simmons,<sup>126</sup>  $\Delta R/R = \{2 - [E/(-dE/dx)]\} \Delta I_{Al}/I_{Al}$ , and further corrected for multiple scattering. The resulting curve passes close to the point determined by Hubbard and MacKenzie<sup>127</sup> at 18 Mev, which is not surprising, since their range determination, when corrected for multiple scattering, yields  $I_{Al} = 165$ , if Simmons formula is used. Further confirmation of the curve is obtained by the recent work of Bichsel and Mozley,<sup>128</sup> whose range point at 17.85 Mev gives  $I_{Al} = 162$  from Simmons formula. Additional support is given by the work of Bloembergen and Van Heerden,<sup>129</sup> who get  $I_{Al} = 161$  and 164 at higher energies. It seems that perhaps the best established range-energy relation is that for 18-Mev protons in Al, and since the p-p protons at  $20^\circ$  had an energy of 18 Mev, it seems safe to take the error of  $\pm 3 \text{ ev}$  in  $I_{Al}$  of reference 123 as the error in the range-energy relation.

As to the second uncertainty in the energy, the extent of energy spread in the beam, only an upper limit can be given. The integral range curves could be fitted quite well by considering just range straggling<sup>103</sup> and angular resolution (cf. p. 43), plus a small low energy tail, due to slit penetration. Similarly, measurements by another method on the beam itself showed no spread other than that expected from straggling. It is believed that an energy spread larger than 0.1 Mev could have been detected.

An upper limit can also be placed on the third uncertainty in the energy, that due to changes in mean energy with time. To minimize such changes, the current regulation of the cyclotron magnet was continually monitored during a run with a Leeds and Northrup Potentiometer. An indication of the constancy of the beam energy under normal conditions is given by the agreement of the energy measurement taken (for  $25^\circ$  p-p) prior to the period of gathering p-d scattering data with that obtained (at  $20^\circ$ ) toward the end of that period. The two values

are 20.56 and 20.57 Mev. The upper limit on the change can be set by the third energy measurement, which was made after the direction of the external beam had shifted (cf. p. 39). This shift caused the collimator to select a different part of the beam, making the mean energy 0.11 Mev higher. Since none of the data taken just before this energy measurement were used, the maximum change in mean energy which could have occurred for any accepted data can be taken as about .08 Mev.

The uncertainty in the mean energy for all the cross section data can be considered as the quadratic addition of the error in the mean energy determination (.08 Mev) and the maximum uncertainty in the change of the mean energy with time (also .08 Mev), giving .11 Mev as the standard deviation in the value of the mean energy. Furthermore, the energy spread in the beam at any time, considered as the standard deviation of the beam energy distribution, is believed not to have exceeded that value of .11 Mev. We then have as the beam energy,  $20.57 \pm .11$  Mev.

#### D. Conclusions

The results of this experiment, which are given in Table IV and Fig. 6, seem a reasonable interpolation between the experimental work at 9.712 and 3113 Mev, except for the appearance of the coulomb-nuclear interference minimum. While it should soon be possible to compare this experiment with the theoretical work<sup>130</sup> of Massey and of Gammel, at the moment the only comparison that can be made is with the 20-Mev n-d calculation of Verde.<sup>74</sup> Although a phase shift analysis ought to be made, the phase shifts converted to equivalent n-d ones (cf. p. 2), and these compared with Verde's phase shifts for each angular momentum, by just comparing cross section curves it is hard to see how the present data could yield phase shifts having any agreement with those of Verde. For either his symmetric or neutral theory, the main cross section minimum comes at too small an angle (about 90°, instead of 130°) and is not deep enough by an order of magnitude. Also the backward peaks are four to six times too high. The forward peak at about 30°, where coulomb effects are not important, is a factor of two too low for the symmetric theory and a factor of one and a half too high for the neutral theory.

Except for checking various theoretical approaches, the data probably cannot yet be used for achieving some of the aims outlined in the Introduction. It can only be hoped that the experiment may provide some spur for the necessary theoretical work. The data can perhaps give an answer to the long-standing question as to which set of nucleon-deuteron scattering lengths is the correct one (cf. p. 2), because of the clear appearance for the first time of a coulomb-nuclear interference minimum. This minimum should give the added condition needed to make unique the phase shifts used to fit the data. In general, this experiment should provide a more stringent test for present or future theories than do previous low or intermediate energy nucleon-deuteron scatterings.

Table IV. Experimental Data

The following data for the angular distribution of protons elastically scattered from deuterons is for a proton laboratory energy of  $20.57 \pm .11$  Mev. The errors, as well as the differential cross section values, are absolute, and are expressed as percentage standard deviations.

Lab. Angle (degrees)	C.M. Angle (degrees)	C.M. Cross Section (mb/sterad.)	Per cent Statistics	Std. Error (per cent)
8.0-p	12.07	93.92	2.7	3.1
10.0-p	15.03	72.93	1.2*	1.8
12.5-p	18.80	69.56	1.4	1.7
15.0-p	22.53	72.37	.93*	1.2
17.5-p	26.26	75.22	.83*	1.1
20.0-p	29.97	77.27	.53	.83
25.0-p	37.37	70.77	.89	1.1
35.0-p	51.87	52.19	.90	1.0
45.0-p	65.95	36.11	.83*	.96
55.0-p	79.44	23.27	1.3	1.4
45.0-d	89.86	16.70	1.4	1.7
65.0-p	92.20	15.49	1.8	1.9
75.0-p	104.17	9.66	1.8	1.9
85.0-p	115.16	5.62	2.8	2.9
90.0-p	120.20	4.51	2.1	2.2
25.0-d	129.90	2.64	2.8	3.1
20.0-d	139.91	6.62	1.5	1.9
17.5-d	144.92	11.44	1.2	1.4
15.0-d	149.93	16.97	1.5	1.9
12.5-d	154.94	24.28	.84	1.3
10.0-d	159.95	33.24	1.9	2.5
8.0-d	163.96	38.65	4.1*	4.3

Proton-proton scattering check run:

20 0	40.20	24.00	.75	1.1
------	-------	-------	-----	-----

\* An additional error due to the background had to be included in the statistical error because of the method of combining sets of data.

## BIBLIOGRAPHY

1. Zimmerman, Cooper, and Frisch, Phys. Rev. 90, 339(A) (1953).  
Details of the energy used have not been published.
2. R. F. Taschek, Phys. Rev. 61, 13 (1942).
3. Brown, Freier, Holmgren, Stratton, and Yarnell, Phys. Rev. 88, 253 (1952).
4. Sherr, Blair, Kratz, Bailey, and Taschek, Phys. Rev. 72, 662 (1947)
5. Tuve, Heydenburg, and Hafstad, Phys. Rev. 50, 806 (1936).
6. Heitler, May, and Powell, Proc. Roy. Soc. (London) A190, 180 (1947).
7. Burrows, Gibson, and Rotblat, Proc. Roy. Soc. (London) A209, 489 (1951).
8. Rodgers, Leiter, and Kruger, Phys. Rev. 78, 656 (1950).
9. Karr, Bondelid, and Mather, Phys. Rev. 81, 37 (1951).
10. K. B. Mather, Phys. Rev. 88, 1408 (1952).
11. L. Rosen and J. C. Allred, Phys. Rev. 82, 777 (1951).
12. Armstrong, Allred, Bondelid, and Rosen, Phys. Rev. 88, 433 (1952).
13. V. J. Ashby, UCRL-2091 (1953), unpublished.
14. M. O. Stern and A. L. Bloom, Phys. Rev. 83, 178 (1951).
15. M. O. Stern, Phys. Rev. 85, 752(A) (1952).
16. A. Bratenahl, UCRL-1852 (1952), unpublished.
17. Cassels, Stafford, and Pickavance, Nature 168, 556 (1951).
18. R. D. Schamberger, Phys. Rev. 85, 424 (1952).
19. D. D. Clark and O. Chamberlain, Bull. Am. Phys. Soc. 29, No. 1, 48 (1954).
20. D. G. Hurst and N. Z. Alcock, Can. J. Phys. 29, 36 (1951).
21. P. R. Tunncliffe, Phys. Rev. 89, 1247 (1953).



22. Adair, Okazaki, and Walt, Phys. Rev. 89, 1165 (1953).
23. A. M. Thorndike and A. W. Watring, Phys. Rev. 82, 295(A) (1951).
24. J. H. Coon and H. H. Barschall, Phys. Rev. 70, 592 (1946).
25. J. H. Darby and J. B. Swann, Australian J. Sci. Research A1, 18 (1948) and Nature 161, 22 (1948).
26. Kruger, Shoupp, Watson, and Stallman, Phys. Rev. 53, 1014 (1938).
27. Martin, Burhop, Alcock, and Boyd, Proc. Phys. Soc. (London) A63, 884 (1950).
28. W. F. Caplehorn and G. P. Rundle, Proc. Phys. Soc. (London) A64, 546 (1951).
29. J. Sanada and S. Yamabe, Phys. Rev. 80, 750 (1950).
30. Hamouda, Halter, and Scherrer, Phys. Rev. 79, 539 (1950) and Helv. Phys. Acta 24, 217 (1951).
31. I. Hamouda and G. Montmoulin, Phys. Rev. 83, 1277 (1951) and Helv. Phys. Acta 25, 107 (1952).
32. E. Wantuch, Phys. Rev. 84, 169 (1951).
33. T. C. Griffith, Proc. Phys. Soc. (London) A66, 894 (1953).
34. Griffith, Remley, and Kruger, Phys. Rev. 79, 443 (1950).
35. J. H. Coon and R. F. Taschek, Phys. Rev. 76, 710 (1949).
36. Armstrong, Allred, and Rosen, Phys. Rev. 91, 90 (1953).
37. Hartsough, Hill, and Powell, Phys. Rev. 79, 219(A) (1950).
38. W. Barkas and M. White, Phys. Rev. 56, 788 (1939).
39. J. H. Gammel, Phys. Rev. 92, 1092(A) (1953).
40. A. L. Bloom, Phys. Rev. 85, 752(A) (1952).
41. J. Hofmann and K. Strauch, Phys. Rev. 90, 449 (1953).
42. Cladis, Hess, and Moyer, Phys. Rev. 87, 425 (1952).
43. Ageno, Amaldi, Bocciaelli, and Trabacchi, Phys. Rev. 71, 20 (1947)
44. J. Hadley, UCRL-1542 (1951), unpublished.

45. L. I. Schiff, Phys. Rev. 52, 149 (1937).
46. H. Primakoff, Phys. Rev. 52, 1000 (1937).
47. K. Ochiai, Phys. Rev. 52, 1221 (1937).
48. S. Flügge, Z. Phys. 108, 545 (1938).
49. L. Motz and J. Schwinger, Phys. Rev. 58, 26 (1940).
50. W. Kohn, Phys. Rev. 74, 1763 (1948).
51. R. Kolodziejski, Nature 165, 110 (1950).
52. S. Borowitz and B. Friedman, Phys. Rev. 89, 441 (1953).
53. S. Tamor, Phys. Rev. 93, 227 (1954).
54. M. M. Gordon, Phys. Rev. 80, 1111 (1950).
55. F. G. Prohammer and T. A. Welton, ONRL-1005 (1951), unpublished.
56. A. Troesch and M. Verde, Helv. Phys. Acta 24, 39 (1951).
57. E. Clementel, Nuovo Cimento 8, 185 (1951).
58. T. Y. Wu and J. Ashkin, Phys. Rev. 73, 986 (1948).
59. G. F. Chew, Phys. Rev. 74, 809 (1948).
60. F. de Hoffmann, Phys. Rev. 78, 216 (1950).
61. G. F. Chew, Phys. Rev. 80, 196 (1950).
62. R. L. Gluckstern and H. A. Bethe, Phys. Rev. 81, 761 (1951).
63. G. F. Chew, Phys. Rev. 84, 710 (1951).
64. G. F. Chew, Phys. Rev. 84, 1057 (1951).
65. B. H. Bransden, Proc. Roy. Soc. (London) A209, 380 (1951).
66. Horie, Tamura, and Yoshida, Prog. Theo. Phys. 6, 623 (1951),  
and Prog. Theo. Phys. 8, 341 (1952).
67. I. Ya. Pomeranchuk, Zh. Eksper. Teor. Fiz. 21, 1113 (1951) and  
Zh. Eksper. Teor. Fiz. 22, 624 (1952).
68. P. B. Daitch and J. B. French, Phys. Rev. 85, 695 (1952).
69. I. L. Karp, Phys. Rev. 85, 754(A) (1952).

70. B. H. Bransden, Proc. Phys. Soc. (London) A65, 972 (1952).
71. J. L. Gammel, Phys. Rev. 92, 1092(A) (1953).
72. R. A. Buckingham and H. S. W. Massey, Proc. Roy. Soc. (London) A179, 123 (1941).
73. H. S. W. Massey and R. A. Buckingham, Phys. Rev. 71, 558 (1947).
74. M. Verde, Helv. Phys. Acta 22, 339 (1949).
75. M. M. Gordon and W. D. Barfield, Phys. Rev. 86, 679 (1952).
76. A. H. de Borde and H. S. W. Massey, as quoted in Progress in Nuclear Physics, Vol. 3, Pergamon Press Ltd., London (1953), pp. 267-268.
77. C. L. Critchfield, Phys. Rev. 73, 1 (1948).
78. H. S. W. Massey and R. A. Buckingham, Phys. Rev. 73, 260 (1948).
79. R. Thomas, Phys. Rev. 76, 1002 (1949).
80. J. L. Gammel, Phys. Rev. 78, 321(A) (1950) and Ph.D. Thesis, Cornell University (1950), unpublished.
81. G. Briet, Phys. Rev. 80, 1110 (1950).
82. Buckingham, Hubbard, and Massey, Proc. Roy. Soc. (London) A211, 183 (1952).
83. A. L. Latter and R. Latter, Phys. Rev. 86, 727 (1952).
84. R. S. Christian and J. L. Gammel, Phys. Rev. 91, 100 (1953).
85. H. H $\ddot{o}$ cker, Physik. Z. 43, 236 (1942).
86. B. H. Bransden and E. H. S. Burhop, Proc. Phys. Soc. (London) A63, 1337 (1950).
87. R. M. Frank and J. L. Gammel, Phys. Rev. 93, 463 (1954).
88. Private communications from Dr. John Brolley (Los Alamos) and Dr. E. O. Salant (Brookhaven).
89. Wollan, Shull, and Koehler, Phys. Rev. 83, 700 (1951).
90. S. D. Drell and K. Huang, Phys. Rev. 91, 1527 (1953).
91. M. M. L $\acute{e}$ vy, Phys. Rev. 88, 725 (1952).
92. A. Klein, Phys. Rev. 89, 1158 (1953).

93. A. Martin and L. Verlet, *Phys. Rev.* 89, 519 (1953).
94. G. Wentzel, *Helv. Phys. Acta*, 25, 569 (1952) and *Phys. Rev.* 91, 1573 (1953).
95. N. Bohr, *Phil. Mag.* 30, 581 (1915) and *Kgl. Danske Videnskab. Selskab, Mat.-fys. Medd* 18, 8 (1948).
96. E. J. Williams, *Proc. Roy. Soc. (London)* A125, 420 (1929).
97. L. Landau, *J. Phys. (U.S.S.R.)* 8, 201 (1944).
98. O. Blunck and S. Leisegang, *Z. Physik* 128, 500 (1950).
99. W. Shultz, *Z. Physik* 129, 530 (1951).
100. K. R. Symon, Ph.D. Thesis, Harvard University (1948), as quoted by B. Rossi, High Energy Particles, Prentice-Hall, New York (1952), pp. 32-35.
101. R. R. Wilson and E. C. Creutz, *Phys. Rev.* 71, 339 (1947).
102. Wilson, Lofgren, Richardson, Wright, and Shankland, *Phys. Rev.* 72, 1131 (1947).
103. D. O. Caldwell, *Phys. Rev.* 88, 131 (1952) and in more detail in D. O. Caldwell, U.C.L.A. Technical Report No. 9. (1952).
104. B. Rossi and K. Greisen, *Rev. Mod. Phys.* 13, 267 (1941).
105. W. C. Dickinson and D. C. Dodder, *Rev. Sci. Instr.* 24, 428 (1953); actual calculations were made according to W. C. Dickinson and D. C. Dodder, LA-1182 (1950), unpublished.
106. W. T. Scott, *Phys. Rev.* 85, 245 (1952).
107. B. Rossi and H. Staub, Ionization Chambers and Counters, McGraw-Hill Book Company, Inc., New York (1949), p. 14.
108. D. H. Wilkinson, Ionization Chambers and Counters, Cambridge University Press, Cambridge (1950), pp. 118-119, 128.
109. W. H. Jordan and P. R. Bell, *Rev. Sci. Instr.* 18, 703 (1947) and Magee, Bell, and Jordan, *Rev. Sci. Instr.* 23, 30 (1952).
110. R. Weissman, *Electronics* 22, 84 (1949).
111. J. L. Yntema and M. G. White, NYO-3478 (1952), unpublished.
112. Worthington, McGruer, and Findley, *Phys. Rev.* 90, 899 (1953).
113. Igo, Clark, and Eisberg, *Phys. Rev.* 89, 879 (1953), and UCRL-2031 (1952).

- 114. W. K. H. Panofsky and F. Fillmore, Phys. Rev. 79, 57 (1950);  
Cork, Johnston, and Richman, Phys. Rev. 79, 71 (1950).
- 115. N. Feather, Proc. Cambridge Phil. Soc. 45, 648 (1949).
- 116. M. M. Shapiro, Phys. Rev. 90, 171 (1953).
- 117. B. L. Cohen and R. V. Neidigh, Phys. Rev. 93, 282 (1954).
- 118. J. W. Burkgig and B. T. Wright, Phys. Rev. 82, 451 (1951); data  
fitted theoretically by Roger Woods (private communication).
- 119. Baker, Dodd, and Simmons, Phys. Rev. 85, 1051 (1952);  
D. H. Simmons, Ph.D. Thesis, Birmingham University (1952),  
unpublished.
- 120. Mass. Inst. of Tech. Lab. for Nuclear Sci. and Eng. Progress  
Report (July 1, 1950), unpublished.
- 121. E. D. Courant, Rev. Sci. Instr. 22, 1003 (1951).
- 122. J. W. M. DuMond and E. R. Cohen, Rev. Mod. Phys. 25, 691 (1953).
- 123. D. O. Caldwell and J. R. Richardson, Phys. Rev. 94, 79 (1954).
- 124. D. C. Sachs and J. R. Richardson, Phys. Rev. 63, 839 (1951) and  
Phys. Rev. 89, 1163 (1953).
- 125. J. H. Smith, Phys. Rev. 71, 32 (1947).
- 126. D. H. Simmons, Proc. Phys. Soc. (London) A65, 454 (1952).
- 127. E. L. Hubbard and K. R. MacKenzie, Phys. Rev. 85, 107 (1952).
- 128. H. Bichsel and R. F. Mozley, Bull. Am. Phys. Soc. 29, #1, 27  
(1954).
- 129. N. Bloembergen and P. J. Van Heerden, Phys. Rev. 83, 561 (1951).
- 130. Private communications from Prof. H. S. W. Massey and Dr.  
J. L. Gammel.

## APPENDIX

A. Counter angle relations

Definitions:

 $\theta_o$  = scattered proton laboratory angle $\alpha_o$  = recoil deuteron laboratory angle (see Fig. 1) $\theta$  = center of mass angle for either the proton or the deuteron (again, see Fig. 1) $m_1$  = mass of the incident particle $m_2$  = mass of the target particle $U = m_1/m_2$  $E$  = energy of the incident particle in the laboratory system $c$  = velocity of light $\beta = (E^2 + 2m_1c^2E)^{1/2} / (E + m_1c^2 + m_2c^2)$  $\mu = [E + m_1c^2(1 + U)] / (E + m_1c^2 + m_2c^2)$ 

Classical equations:

$$\tan \theta_o = (\sin \theta) / (U + \cos \theta) = \sin 2\alpha_o / (U - \cos 2\alpha_o)$$

$$\alpha_o = (\pi - \theta) / 2$$

Relativistic equations:

$$\tan \theta_o = (\sqrt{1 - \beta^2} \sin \theta) / (\mu + \cos \theta)$$

$$\tan \alpha_o = \sqrt{1 - \beta^2} \cot \theta / 2$$

B. Variation of particle energy with laboratory angle

Definitions as above, with the addition of

 $E_S$  = energy of the scattered particle $E_R$  = energy of the recoil particle $E' = E / (m_1c^2)$  $V = 1/U = m_2/m_1$

Classical equations:

$$E_S = [E/(m_1 + m_2)^2][m_2^2 + m_1^2 (2 \cos^2 \theta_0 - 1) + 2m_1 \cos \theta_0 \sqrt{m_2^2 - m_1^2 \sin^2 \theta_0}]$$

$$E_R = 4Em_1m_2 \cos^2 \alpha_0 / (m_1 + m_2)^2$$

Relativistic equations:

$$E_S = m_1 c^2 \left\{ \frac{(E' + V + 1) [1 + V(E' + 1)] + E'(E' + 2) \cos \theta_0 \sqrt{V^2 - \sin^2 \theta_0}}{(E' + V + 1)^2 - E'(E' + 2) \cos^2 \theta_0} - 1 \right\}$$

$$E_R = (m_2 c^2) \frac{2 E' (E' + 2) \cos^2 \alpha_0}{(E' + V + 1)^2 - E' (E' + 2) \cos^2 \alpha_0}$$

To find, classically, the maximum energy at a given laboratory angle which a proton from the disintegration of the deuteron,  $D(p, 2p)N$ , can have, we consider the case in which a proton and a neutron go off in one direction and the high energy proton goes off in the opposite direction (in the center of mass system). If the binding energy of the deuteron is  $W$  ( $= -2.226$  Mev), then this maximum energy is

$$E_M = (E/9)[2 \cos^2 \theta_0 + 2 \cos \theta_0 \sqrt{\cos^2 \theta_0 + 3 + 6W/E} + 3 + 6W/E]$$

### C. Transformation of laboratory to center of mass cross sections

Definitions as above, with the addition of

$\sigma_0(\theta_0)$  = differential cross section in the laboratory system

$\sigma(\theta)$  = differential cross section in the center of mass system

$$B = \frac{\sigma(\theta)}{\sigma_0(\theta_0)} = \frac{\sin \theta_0 d\theta_0}{\sin \theta d\theta} \quad (\text{with } B_S \text{ for the scattered particle and } B_R \text{ for the recoil particle})$$

Classical equations:

$$B_S = |1 + U \cos \theta| / (1 + U^2 + 2U \cos \theta)^{3/2}$$

$$B_R = 1 / (4 \cos \alpha_0)$$



Relativistic equations:

$$B_S = (1 - \beta^2) (1 + \mu \cos \theta) / [\mu^2 + 2\mu \cos \theta + 1 - \beta^2 \sin^2 \theta]^{3/2}$$

$$B_R = (1 - \beta^2 \cos^2 \alpha_0)^2 / [4(1 - \beta^2) \cos \alpha_0]$$

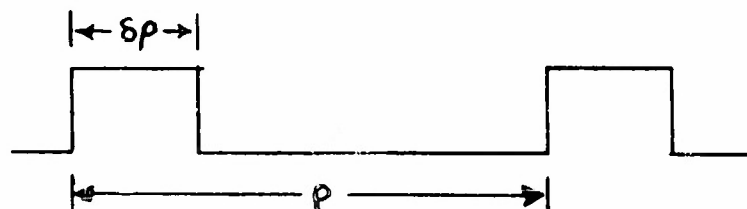
#### D. Accidental coincidences with a pulsed source

The mean accidental counting rate for  $n$  counters of resolving time  $\tau$  and with individual mean counting rates  $R_1, R_2, \dots, R_n$  when used with a square-pulsed beam of period  $p$  and on-time  $\delta p$  was found to be  $A_R = n R_1 R_2 \dots R_n \tau^{n-1} [\delta^{1-n} (n-1) \tau / (n p \delta^n)]$ .

If we deal with the total number of counts in a time  $t$ , then  $N_n = R_n t$ , and the total number of accidental counts is

$$A_N = n N_1 N_2 \dots N_n (\tau/t)^{n-1} [\delta^{1-n} (n-1) \tau / (n p \delta^n)].$$

If  $A_E$  is found experimentally by introducing delays into each counting channel but one and recording the resulting coincidences, the number found will be too small if the longest delay,  $d$ , is an appreciable fraction of  $\delta p$ . The correct  $A (= A_N \text{ or } A_R)$  for a square beam pulse is  $A = A_E \delta p / (\delta p - d)$ .



#### E. Finite beam size correction

Definitions:

$\sigma_o(\theta_o)$  = differential cross section in the laboratory system as determined assuming incident and scattered beams of infinitesimal thickness.

$\sigma'_o(\theta_o)$  and  $\sigma''_o(\theta_o)$  = the first and second derivatives with respect to angle of  $\sigma_o(\theta_o)$ .

$D_F$  = width of the first (front) analyzing slit

$D_R$  = width of the second (rear) analyzing slit

$H$  = height of the rear analyzing slit

$r_1$  = distance between the slits

$r_2$  = distance from the scattering center to the rear slit

$w$  = half-width of the incident beam at the scattering center

$L$  = distance from the apex of the cone to the scattering center, if the incident beam is assumed to be conical.

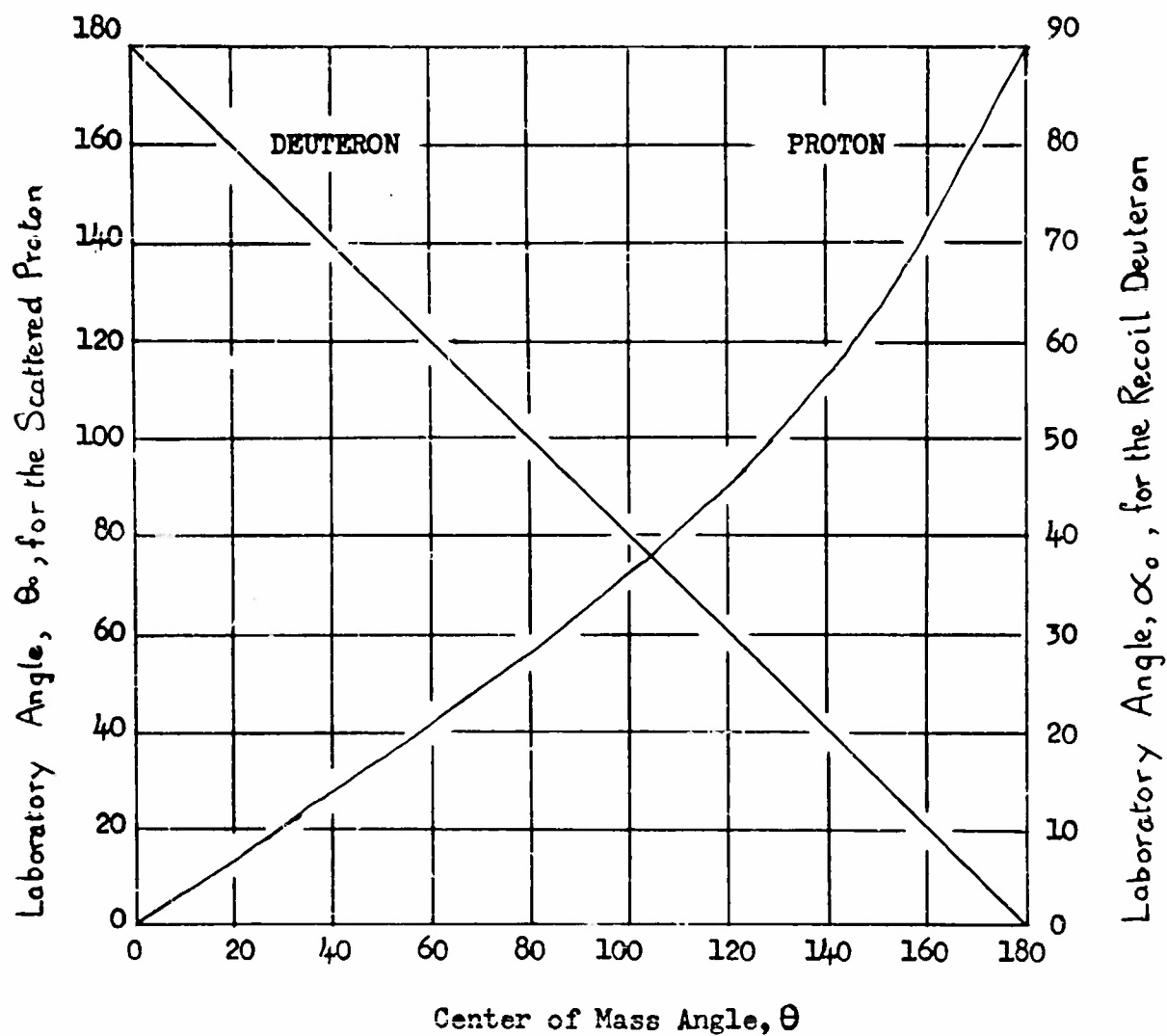
The corrected cross section was obtained by dividing  $\sigma_o(\theta_o)$  by

$$1 - \frac{D_F^2 + D_R^2}{8r_1^2} - \frac{3w^2 + H^2}{8r_2^2} + \frac{w^2}{4r_2^2 \sin^2 \theta_o} + \frac{D_R^2}{12r_2^2} \cot^2 \theta_o + \frac{7}{640} \frac{H^4}{r_2^4} \\ + \frac{\sigma_o'(\theta_o)}{\sigma_o(\theta_o)} \left( \frac{3w^2 + H^2}{24r_2^2} - \frac{D_R^2}{12r_1 r_2} - \frac{9}{640} \frac{H^4}{r_2^4} + \frac{\gamma}{3} \right) \cot \theta_o \\ + \frac{\sigma_o''(\theta_o)}{\sigma_o(\theta_o)} \left( \frac{D_F^2 + D_R^2}{24r_1^2} + \frac{H^4 \cot^2 \theta_o}{640r_2^4} \right).$$

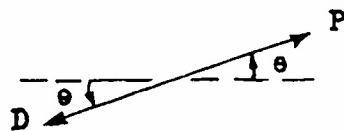
$$\text{where } \gamma = \frac{1}{L^2 \sin^2 \theta_o} \left( r_2^2 \frac{D_F^2 + D_R^2}{12r_1^2} - \frac{r_2 D_R^2}{6r_1} + \frac{D_R^2}{12} \right) + \frac{w^2}{4Lr_2 \cos \theta_o}.$$

The correction without the  $\gamma$  term is for a cylindrical incident beam, while that with a full  $\gamma$  term is for a conical incident beam. Using 1/3 of the small  $\gamma$  term was considered to represent the actual beam best.

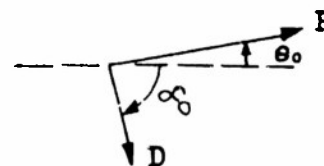
This correction, except for the choice of the  $\gamma$  coefficient and for the terms in  $H^4/r_2^4$  which had to be included because of the relatively large size of  $H$  in this experiment, was derived by Prof. C. L. Critchfield.



Angles are measured as shown:

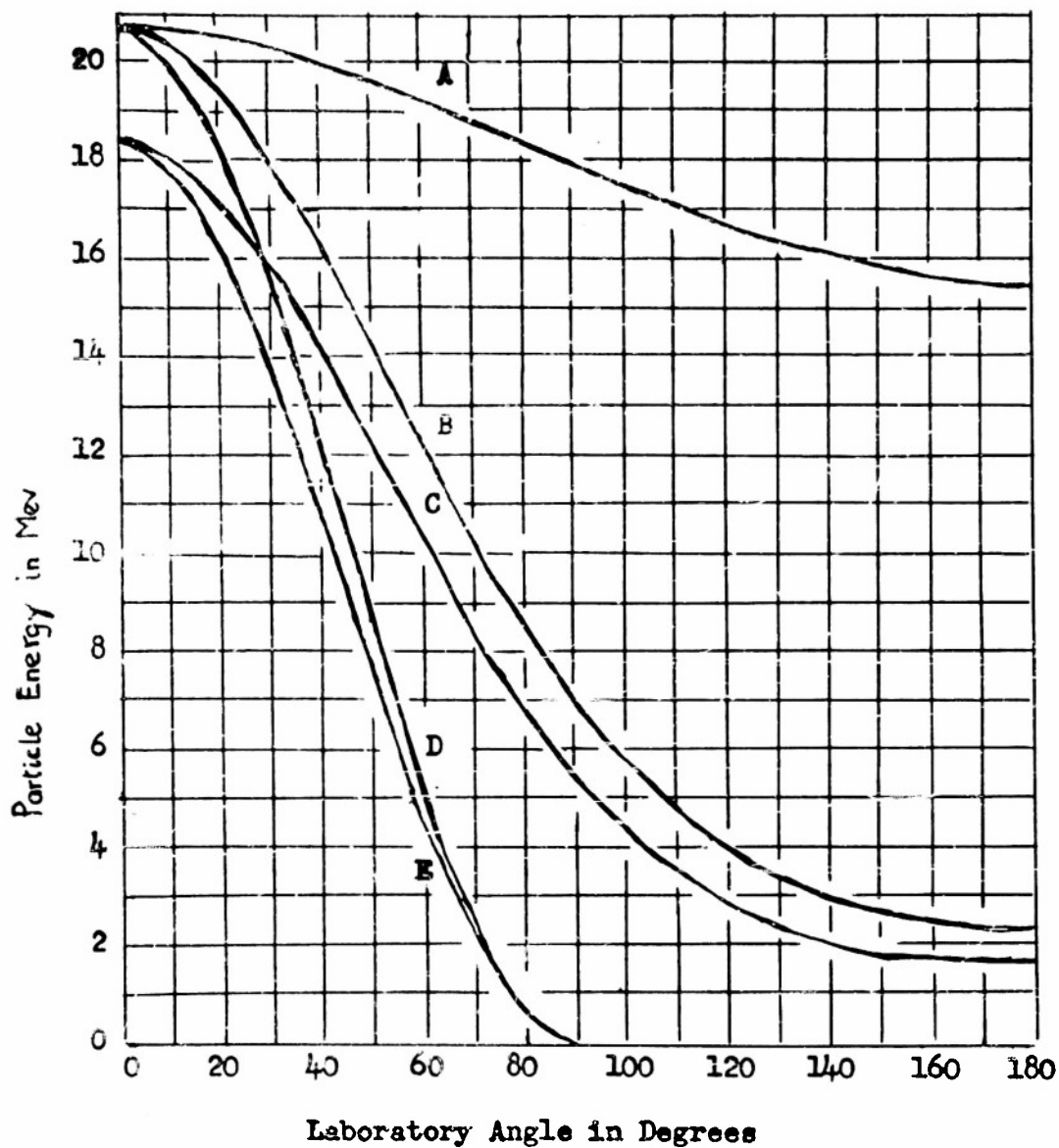


Center of Mass



Laboratory

Figure 1 - LABORATORY ANGLES vs. CENTER OF MASS ANGLE



- Curve A: PROTONS SCATTERED from NITROGEN  
Curve B: PROTONS SCATTERED from DEUTERIUM  
Curve C: MAXIMUM ENERGY PROTONS from D (p, 2p) N  
Curve D: PROTONS SCATTERED from HYDROGEN  
Curve E: RECOIL DEUTERONS from p-d SCATTERING

Figure 2 - PARTICLE ENERGY vs. LABORATORY ANGLE

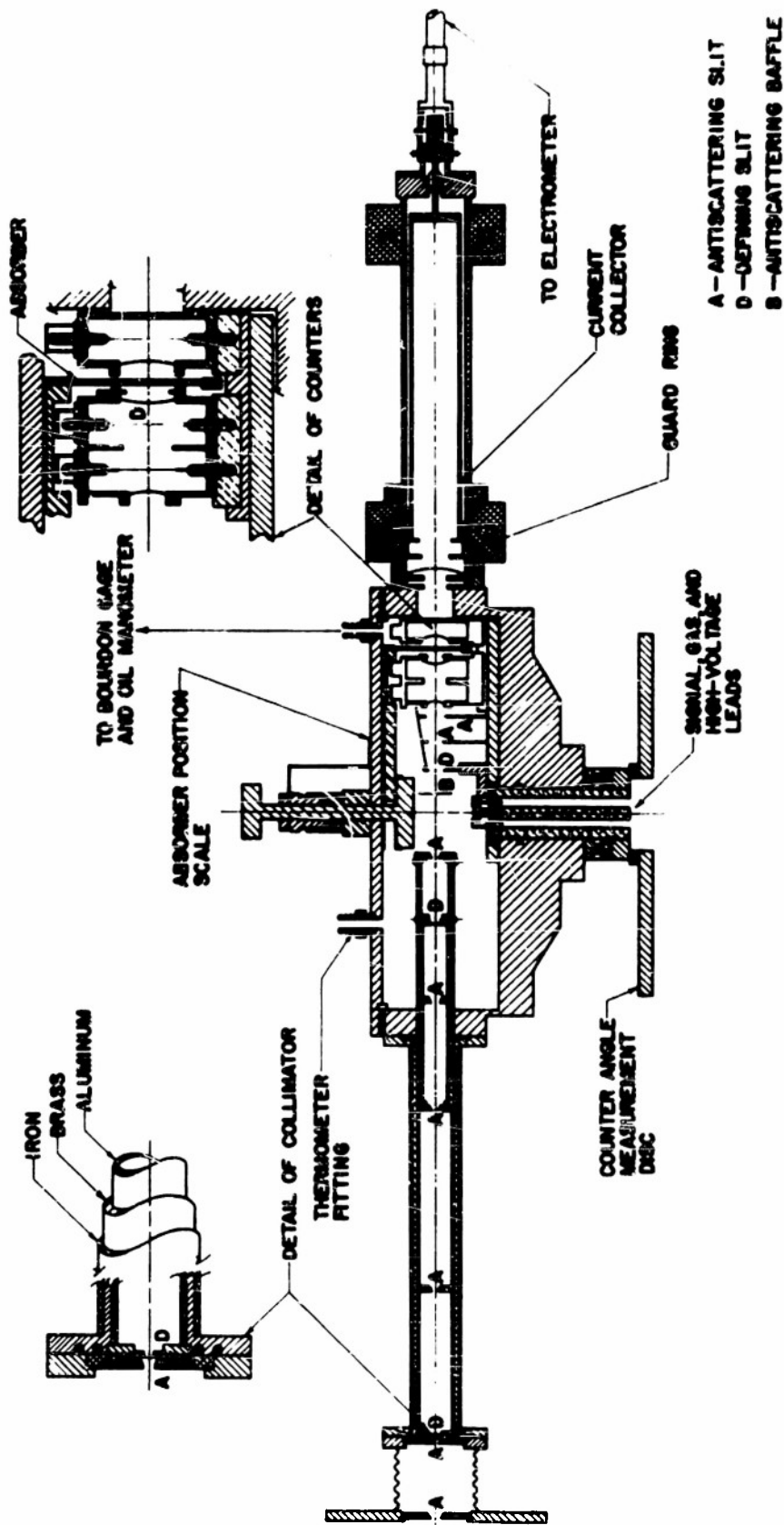
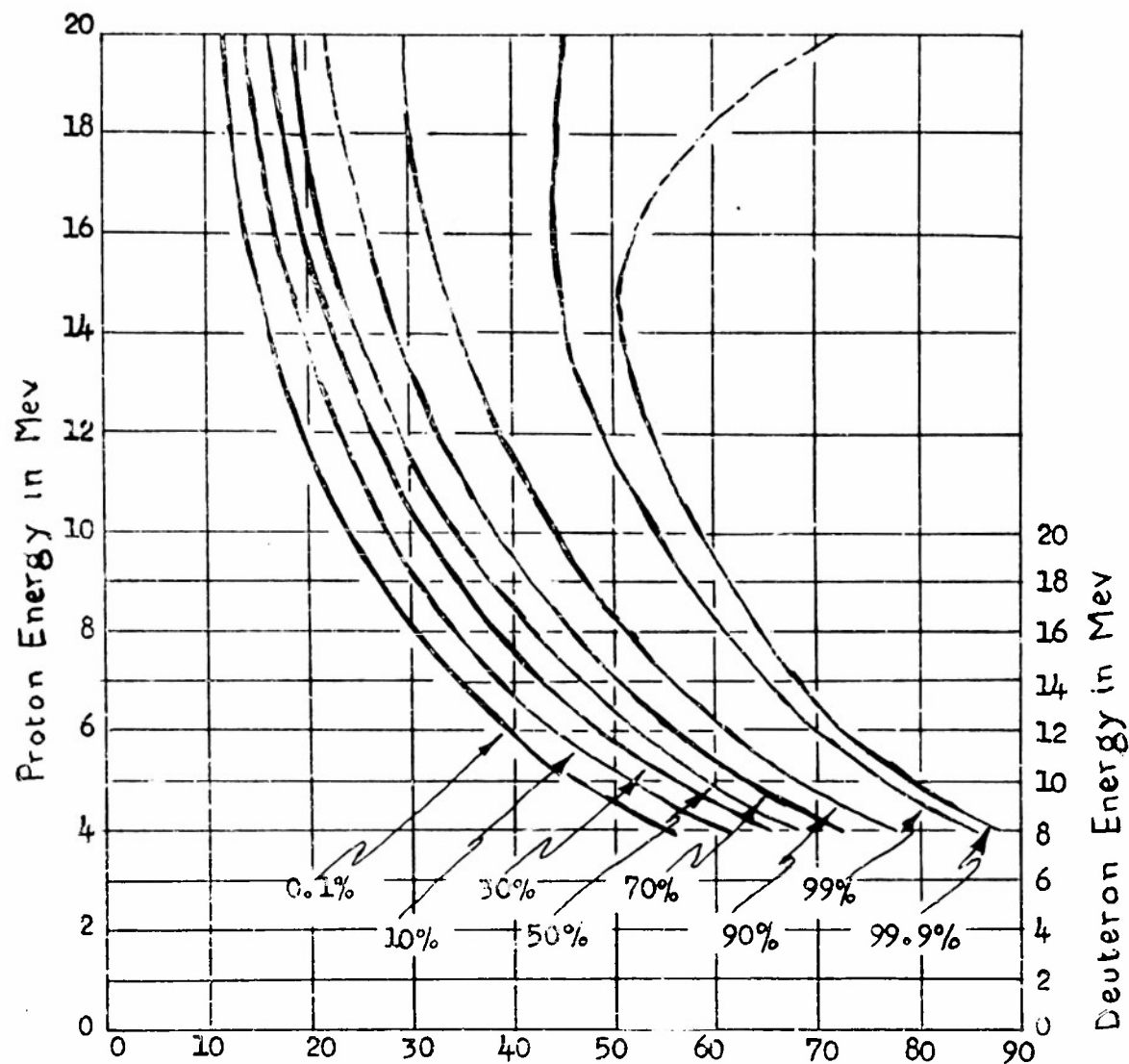


Figure 3 - SECTIONAL VIEW OF THE SCATTERING CHAMBER



Max. Energy Loss in Kev for 1.44 cm. of 1/2 Atm. Argon

For a given percentage of monoenergetic particles, each curve represents the maximum energy loss vs. particle energy.

Figure 4 - ENERGY LOSS DISTRIBUTION IN A COUNTER  
vs. PROTON AND DEUTERON ENERGY

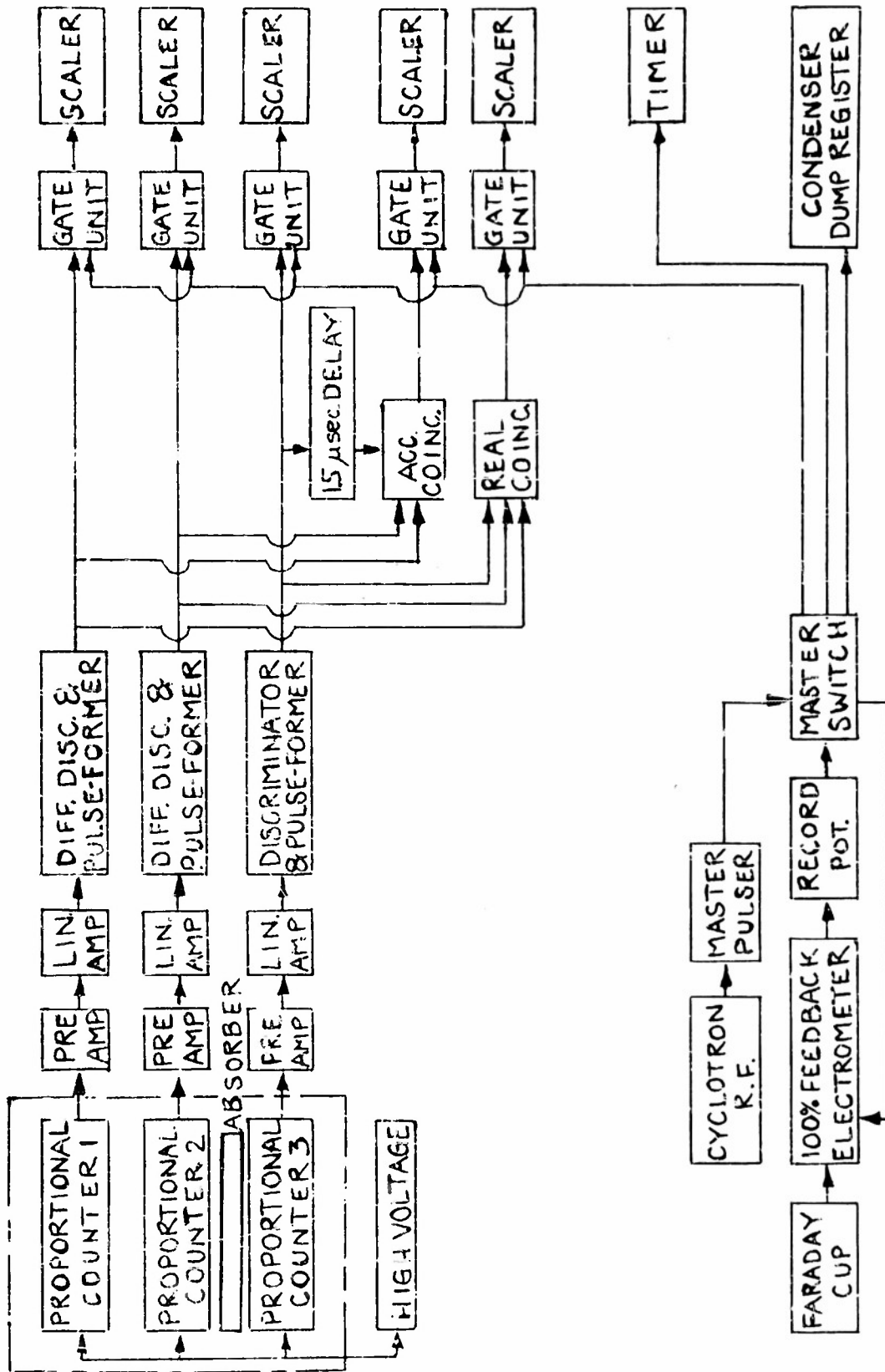


FIGURE 5 - ELECTRONICS BLOCK DIAGRAM



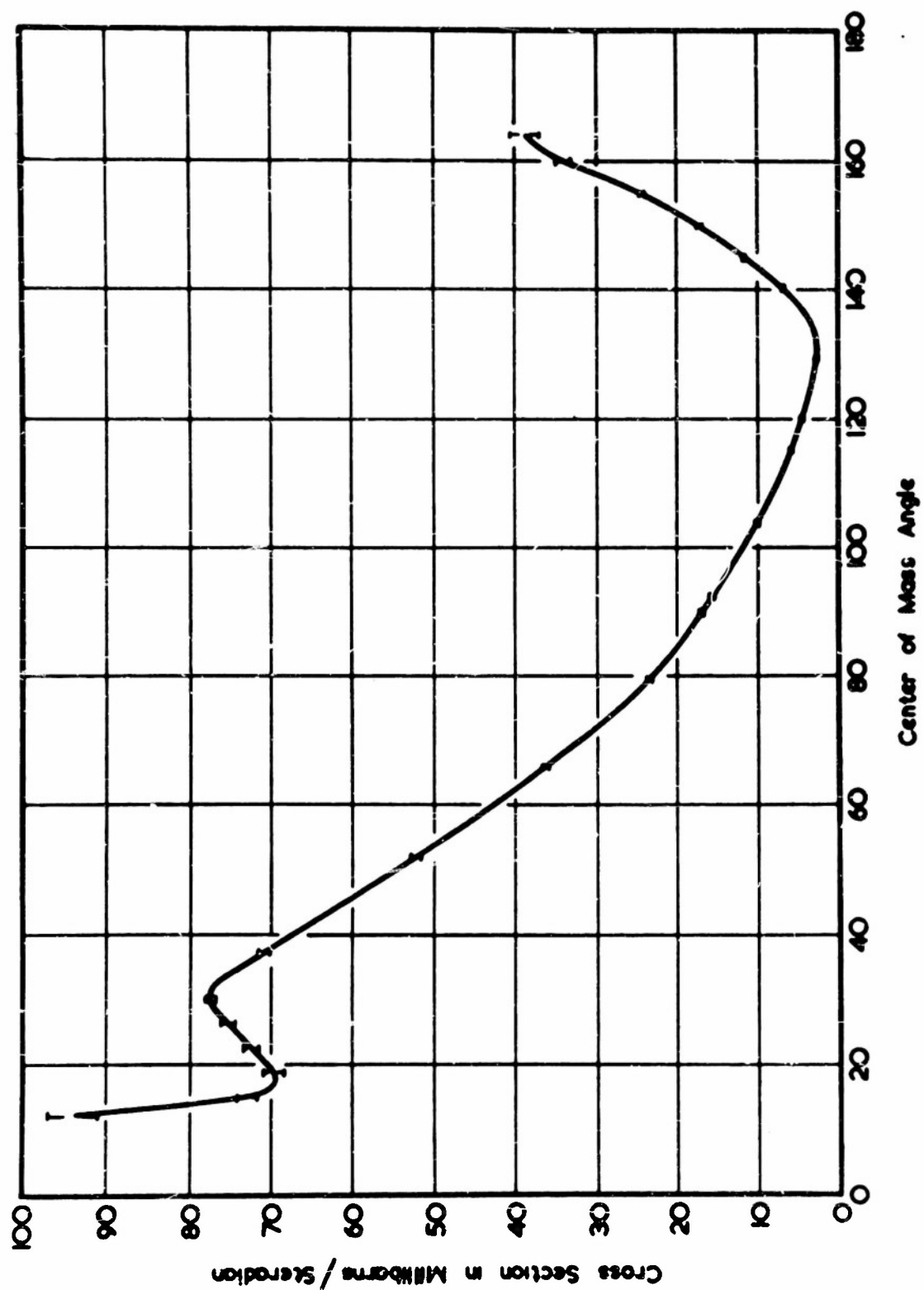


Figure 6 -- DIFFERENTIAL CROSS SECTION for 20.6-MeV p-d ELASTIC SCATTERING.

## DISTRIBUTION LIST

Contract N6onr-275 Task IV

### Professional

Dr. W. F. G. Swann, Director  
Bartol Research Foundation  
Franklin Institute  
Swarthmore, Pennsylvania.

Prof. C. C. Lauritsen  
Department of Physics  
California Institute of Technology  
Pasadena, California.

Prof. C. D. Anderson  
Department of Physics  
California Institute of Technology  
Pasadena, California.

Prof. R. B. Brode  
Department of Physics  
University of California  
Berkeley 4, California

Prof. E. O. Lawrence  
Radiation Laboratory  
University of California  
Berkeley 4, California.

Prof. J. R. Richardson  
Department of Physics  
University of California  
Los Angeles 24, California.

Prof. E. C. Creutz  
Department of Physics  
Carnegie Institute of Technology  
Schenley Park  
Pittsburgh 13, Pennsylvania.

Dr. M. A. Tuve  
Department of Terrestrial Magnetism  
Carnegie Institution of Washington  
Washington, D.C.

Dr. R. S. Shankland  
Case Institute of Technology  
Department of Physics  
University Circle  
Cleveland 6, Ohio.

Prof. S. K. Allison  
Institute of Nuclear Studies  
University of Chicago  
Chicago, Illinois.

Prof. J. Rainwater  
Columbia University  
Nevis Cyclotron Laboratories  
P. O. Box 117  
Irvington-on-Hudson, New York.

Prof. R. R. Wilson  
Laboratory of Nuclear Studies  
Cornell University  
Ithaca, New York.

Prof. W. M. Nielson  
Department of Physics  
Duke University  
Durham, North Carolina

Dr. Guy Suits  
Research Laboratory  
General Electric Company  
Schenectady, New York.

Dr. Zoltan Bay  
Department of Physics  
George Washington University  
Washington, D.C.

Prof. N. F. Ramsey  
Department of Physics  
Harvard University  
Cambridge, Massachusetts.

Director  
Nuclear Laboratory  
Harvard University  
Cambridge, Massachusetts

Prof. F. W. Loomis  
Department of Physics  
University of Illinois  
Urbana, Illinois.

Prof. A. C. G. Mitchell  
Department of Physics  
Indiana University  
Bloomington, Indiana.

Prof. J. A. Van Allen  
Department of Physics  
State University of Iowa  
Iowa City, Iowa.

Prof. J. D. Stranathan  
Department of Physics  
University of Kansas  
Lawrence, Kansas.

Prof. J. M. Cork  
Department of Physics  
University of Michigan  
Ann Arbor, Michigan.

Prof. W. E. Hazen  
Department of Physics  
University of Michigan  
Ann Arbor, Michigan.

Prof. J. H. Williams  
Department of Physics  
University of Minnesota  
Minneapolis, Minnesota.

Prof. E. P. Ney  
Department of Physics  
University of Minnesota  
Minneapolis, Minnesota.

Prof. Truman S. Gray  
Servo-Mechanisms Laboratory  
Massachusetts Institute of Technology  
Cambridge 39, Massachusetts.

Professor J. R. Zacharias .... (2)  
Laboratory for Nuclear Science and  
Engineering  
Massachusetts Institute of Technology  
Cambridge, Massachusetts.

Prof. S. A. Korff  
Department of Physics  
New York University  
University Heights  
New York 53, New York.

Prof. B. Waldman  
Nuclear Physics Laboratory  
University of Notre Dame  
Notre Dame, Indiana.

Prof. J. N. Cooper  
Department of Physics  
Ohio State University  
Columbus 10, Ohio.

Prof. W. E. Stephens  
Department of Physics  
University of Pennsylvania  
Philadelphia 4, Pennsylvania.

Prof. A. J. Allen  
Department of Physics  
University of Pittsburgh  
Pittsburgh, Pennsylvania

Prof. G. T. Reynolds  
Department of Physics  
Princeton University  
Princeton, New Jersey.

Prof. M. G. White  
Department of Physics  
Princeton University  
Princeton, New Jersey.

Prof. Leticia del Rosario  
Department of Physics  
Gobierno de Puerto Rico  
Universidad de Puerto Rico  
Rio Piedras  
Puerto Rico.

Prof. T. W. Bonner  
Department of Physics  
Rice Institute  
Houston, Texas.

Prof. R. E. Marshak  
Department of Physics  
University of Rochester  
Rochester, New York

Prof. Charles A. Whitmer  
Chairman, Department of Physics  
Rutgers University  
New Brunswick, New Jersey.

Prof. E. L. Ginzton  
Microwave Laboratory  
Stanford University  
Palo Alto, California.

Prof. F. Bloch  
Department of Physics  
Stanford University  
Palo Alto, California.

Prof. J. D. Trimmer  
Department of Physics  
University of Tennessee  
Knoxville, Tennessee.

Prof. K. Lark-Horovitz  
Department of Physics  
Purdue University  
Lafayette, Indiana.

Prof. A. L. Hughes  
Department of Physics  
Washington University  
St. Louis, Missouri.

Prof. R. D. Sard  
Department of Physics  
Washington University  
St. Louis, Missouri.

Prof. J. H. Manley  
Department of Physics  
University of Washington  
Seattle 5, Washington.

Dr. J. W. Coltman  
Research Laboratories  
Westinghouse Electric Corp.  
East Pittsburgh, Pennsylvania.

Prof. R. G. Herb  
Department of Physics  
University of Wisconsin  
Madison 6, Wisconsin

Prof. W. M. Watson .... (2)  
Department of Physics  
Sloane Physics Laboratory  
Yale University  
New Haven, Connecticut.

Prof. C. L. Critchfield  
University of Minnesota  
Minneapolis, Minnesota.

Prof. G. Breit  
Yale University  
New Haven, Connecticut.

Prof. Edward Teller  
Physics Department  
University of California  
Berkeley 4, California.

#### Governmental

Chief of Naval Research ..... (2)  
Attn: Nuclear Physics Branch  
Navy Department  
Washington 25, D.C.

Director,  
Naval Research Laboratory.....(9)  
Attn: Technical Information Officer  
Washington 25, D.C.

Director  
Office of Naval Research  
Chicago Branch Office  
844 North Rush Street  
Chicago 11, Illinois.

Director  
Office of Naval Research  
San Francisco Branch Office  
801 Donahue Street  
San Francisco 24, California.

Director  
Office of Naval Research  
New York Branch Office  
346 Broadway  
New York 13, New York.

Director  
Office of Naval Research  
Pasadena Branch Office  
1030 East Green Street  
Pasadena 1, California.

Officer in Charge .....(10)  
Office of Naval Research  
Navy No. 100  
Fleet Post Office  
New York, New York.

Superintendent  
Nucleonics Division  
Naval Research Laboratory  
Anacostia, Washington, D.C.

Chief, Bureau of Ships  
Attn: Code 390  
Navy Department  
Washington 25, D.C.

Chief, Bureau of Ships  
Attn: Code 330  
Navy Department  
Washington 25, D.C.

Chief, Bureau of Ordnance  
Attn: Rem  
Navy Department  
Washington 25, D.C.

Chief, Bureau of Ordnance  
Attn: Reys  
Navy Department  
Washington 25, D.C.

Chief, Bureau of Aeronautics  
Attn: RS-5  
Navy Department  
Washington 25, D.C.

Chief, Bureau of Aeronautics  
Attn: Technical Library  
Navy Department  
Washington 25, D.C.

Commanding Officer  
Naval Radiological Defense Laboratory  
San Francisco Naval Shipyard  
San Francisco 24, California.

Chief of Naval Operations  
Attn: Op30  
Navy Department  
Washington 25, D.C.

Commander  
U.S. Naval Ordnance Test Station  
Technical Library  
Inyokern, China Lake, California.

Commanding General  
Air Force Cambridge Research Center  
Attn: Geophysics Research Library  
230 Albany Street  
Cambridge 39, Massachusetts.

Senior Scientific Adviser  
Office of the Under Secretary of  
the Army  
Department of the Army  
Washington 25, D.C.

Director  
Research and Development Division  
General Staff  
Department of the Army  
Washington 25, D.C.

Chief, Physics Branch  
U.S. Atomic Energy Commission  
1901 Constitution Avenue, N.W.  
Washington 25, D.C.

U. S. Atomic Energy Commission  
Attn: Roland Anderson  
Patent Branch  
1901 Constitution Avenue, N.W.  
Washington 25, D.C.

U. S. Atomic Energy Commission...(4)  
Library Branch  
Technical Information Division, ORE  
P.O. Box E  
Oak Ridge, Tennessee.

Oak Ridge National Laboratory  
Attn: Central Files  
P.O. Box P  
Oak Ridge, Tennessee.

Oak Ridge National Laboratory  
Attn: Head, Physics Division  
P.O. Box P  
Oak Ridge, Tennessee.

Brookhaven National Laboratory  
Attn: Dr. S. C. Stanford  
Research Library  
Upton, L. I., New York.

Argonne National Laboratory  
Attn: Hoyland D. Young  
P. O. Box 5207  
Chicago 80, Illinois.

Document Custodian  
Los Alamos Scientific Lab.  
P.O. Box 1663  
Los Alamos, New Mexico.

Technical Information Group  
General Electric Company  
P.O. Box 100  
Richland, Washington.

Carbide and Carbon Chemical Division  
(K-25 Plant)  
Plant Records Department  
Central Files (K-25)  
P.O. Box P  
Oak Ridge, Tennessee.

Carbide and Carbon Chemical Division  
(Y-12 Plant)  
Central Reports and Information (Y-12)  
P. O. Box P  
Oak Ridge, Tennessee.

Ames Laboratory  
Iowa State College  
P. O. Box 14A, Station A  
Ames, Iowa.

Knolls Atomic Power Laboratory  
Attn: Document Librarian  
P. O. Box 1072  
Schenectady, New York.

Mound Laboratory  
Attn: Dr. M. M. Haring  
U. S. Atomic Energy Commission  
P. O. Box 32  
Miamisburg, Ohio.

Sandia Corporation  
Sandia Base  
Attn: Mr. Dale N. Evans  
Classified Document Division  
Albuquerque, New Mexico.

U. S. Atomic Energy Commission  
Attn: Division of Technical  
Information and Declassifi-  
cation Service  
New York Operations Office  
P.O. Box 30  
Ansonia Station  
New York 23, New York.

National Bureau of Standards  
Library  
Room 203, Northwest Building  
Washington 25, D.C.

National Science Foundation  
2144 California Street  
Washington 25, D.C.

Director, Office of Ordnance  
Research  
2127 Myrtle Drive  
Durham, North Carolina.

Commanding General  
Air Research and Development  
Command  
Attn: RDRRP  
P.O. Box 1395  
Baltimore 3, Maryland.

Dr. John Gammel  
Los Alamos Scientific Lab.  
P.O. Box 1663  
Los Alamos, New Mexico.

Dr. J. M. B. Kellogg  
Los Alamos Scientific Lab.  
P.O. Box 1663  
Los Alamos, New Mexico.

Dr. A. H. Snell  
Oak Ridge National Laboratory  
P.O. Box P  
Oak Ridge, Tennessee.

Foreign

Doctor Cesar Lattes  
Scientific Director  
Brazilian Center of Physical Research  
Rio de Janeiro  
Brazil.

Prof. H. S. W. Massey  
University College  
London University  
Gower Street  
London, W.C.1, England.

Dr. A. H. De Borde  
Glasgow University  
Glasgow, Scotland.

Dr. E. Bretscher  
Atomic Energy Research Establishment  
Harwell  
Didcot, Berks., England.

Dr. Allen  
Atomic Energy Research Establishment  
Harwell  
Didcot, Berks., England.

Prof. P. Scherrer  
Physikalisches Institut  
Eidgenössische Technische Hochschule  
Gloriastrasse 35  
Zürich 7, Switzerland.



# Armed Services Technical Information Agency

Because of our limited supply, you are requested to return this copy WHEN IT HAS SERVED YOUR PURPOSE so that it may be made available to other requesters. Your cooperation will be appreciated.

**AD**

**40814**

NOTICE: WHEN GOVERNMENT OR OTHER DRAWINGS, SPECIFICATIONS OR OTHER DATA ARE USED FOR ANY PURPOSE OTHER THAN IN CONNECTION WITH A DEFINITELY RELATED GOVERNMENT PROCUREMENT OPERATION, THE U. S. GOVERNMENT THEREBY INCURS NO RESPONSIBILITY, NOR ANY OBLIGATION WHATSOEVER; AND THE FACT THAT THE GOVERNMENT MAY HAVE FORMULATED, FURNISHED, OR IN ANY WAY SUPPLIED THE SAID DRAWINGS, SPECIFICATIONS, OR OTHER DATA IS NOT TO BE REGARDED BY IMPLICATION OR OTHERWISE AS IN ANY MANNER LICENSING THE HOLDER OR ANY OTHER PERSON OR CORPORATION, OR CONVEYING ANY RIGHTS OR PERMISSION TO MANUFACTURE, USE OR SELL ANY PATENTED INVENTION THAT MAY IN ANY WAY BE RELATED THERETO.

Reproduced by  
**DOCUMENT SERVICE CENTER**  
KNOTT BUILDING, DAYTON, 2, OHIO

**UNCLASSIFIED**